UNITED STATES AIR FORCE

SUMMER RESEARCH PROGRAM -- 1997

GRADUATE STUDENT RESEARCH PROGRAM FINAL REPORTS

VOLUME 11

ARNOLD ENGINEERING DEVELOPMENT CENTER

UNITED STATES AIR FORCE ACADEMY

WILFORD HALL MEDICAL CENTER

RESEARCH & DEVELOPMENT LABORATORIES

5800 Uplander Way

Culver City, CA 90230-6608

Program Director, RDL
Gary Moore

Program Manager, AFOSR
Major Linda Steel-Goodwin

Program Manager, RDL
Scott Licoscos

Program Administrator, RDL
Johnetta Thompson

Program Administrator, RDL
Rebecca Kelly-Clemmons

Submitted to:

AIR FORCE OFFICE OF SCIENTIFIC RESEARCH

Bolling Air Force Base

Washington, D.C.

December 1997

REPORT DOCUMENTATION PAGE			wed 4-0188
Public reporting burden for this collection of information is estimated to average 1 hour per response, including the time for rev the collection of information. Send comments regarding this burden estimate or any other aspect of this collection of info Operations and Reports, 1215 Jefferson Davis Highway, Suite 1204, Arlington, VA 22202-4302, and to the Office of Manage	AFRL-SR-BL-TR-00- 0767		id, and completing and reviewing ces, Directorate for Information
1. AGENCY USE ONLY *(Leave blank)*	2. REPORT DATE December, 1997		
4. TITLE AND SUBTITLE 1997 Summer Research Program (SRP), Graduate Student Research Program (GSRP), Final Reports, Volume 11, Arnold Eng. Development Center, US Air Force Academy, and Wilford Hall Medical Center			5. FUNDING NUMBERS F49620-93-C-0063
6. AUTHOR(S) Gary Moore			
7. PERFORMING ORGANIZATION NAME(S) AND ADDRESS(ES) Research & Development Laboratories (RDL) 5800 Uplander Way Culver City, CA 90230-6608			8. PERFORMING ORGANIZATION REPORT NUMBER
9. SPONSORING/MONITORING AGENCY NAME(S) AND ADDRESS(ES) Air Force Office of Scientific Research (AFOSR) 801 N. Randolph St. Arlington, VA 22203-1977			10. SPONSORING/MONITORING AGENCY REPORT NUMBER
11. SUPPLEMENTARY NOTES			
12a. DISTRIBUTION AVAILABILITY STATEMENT Approved for Public Release			12b. DISTRIBUTION CODE

13. ABSTRACT *(Maximum 200 words)*

The United States Air Force Summer Research Program (USAF-SRP) is designed to introduce university, college, and technical institute faculty members, graduate students, and high school students to Air Force research. This is accomplished by the faculty members (Summer Faculty Research Program, (SFRP)), graduate students (Graduate Student Research Program (GSRP)), and high school students (High School Apprenticeship Program (HSAP)) being selected on a nationally advertised competitive basis during the summer intersession period to perform research at Air Force Research Laboratory (AFRL) Technical Directorates, Air Force Air Logistics Centers (ALC), and other AF Laboratories. This volume consists of a program overview, program management statistics, and the final technical reports from the GSRP participants at the Arnold Engineering Development Center, US Air Force Academy, and Wilford Hall Medical Center.

14. SUBJECT TERMS			15. NUMBER OF PAGES
Air Force Research, Air Force, Engineering, Laboratories, Reports, Summer, Universities, Faculty, Graduate Student, High School Student			16. PRICE CODE
17. SECURITY CLASSIFICATION OF REPORT	18. SECURITY CLASSIFICATION OF THIS PAGE	19. SECURITY CLASSIFICATION OF ABSTRACT	20. LIMITATION OF ABSTRACT
Unclassified	Unclassified	Unclassified	UL

UNITED STATES AIR FORCE

SUMMER RESEARCH PROGRAM -- 1997

GRADUATE STUDENT RESEARCH PROGRAM FINAL REPORTS

VOLUME 11

ARNOLD ENGINEERING DEVELOPMENT CENTER
UNITED STATES AIR FORCE ACADEMY
WILFORD HALL MEDICAL CENTER

RESEARCH & DEVELOPMENT LABORATORIES

5800 Uplander Way

Culver City, CA 90230-6608

Program Director, RDL
Gary Moore

Program Manager, AFOSR
Major Linda Steel-Goodwin

Program Manager, RDL
Scott Licoscos

Program Administrator, RDL
Johnetta Thompson

Program Administrator, RDL
Rebecca Kelly-Clemmons

Submitted to:

AIR FORCE OFFICE OF SCIENTIFIC RESEARCH

Bolling Air Force Base

Washington, D.C.

December 1997

PREFACE

Reports in this volume are numbered consecutively beginning with number 1. Each report is paginated with the report number followed by consecutive page numbers, e.g., 1-1, 1-2, 1-3; 2-1, 2-2, 2-3.

This document is one of a set of 16 volumes describing the 1997 AFOSR Summer Research Program. The following volumes comprise the set:

VOLUME	**TITLE**
1	Program Management Report
	Summer Faculty Research Program (SFRP) Reports
2A & 2B	Armstrong Laboratory
3A & 3B	Phillips Laboratory
4A & 4B	Rome Laboratory
5A , 5B & 5C	Wright Laboratory
6	Arnold Engineering Development Center, United States Air Force Academy and Air Logistics Centers
	Graduate Student Research Program (GSRP) Reports
7A & 7B	Armstrong Laboratory
8	Phillips Laboratory
9	Rome Laboratory
10A & 10B	Wright Laboratory
11	Arnold Engineering Development Center, United States Air Force Academy, and Wilford Hall Medical Center
	High School Apprenticeship Program (HSAP) Reports
12A & 12B	Armstrong Laboratory
13	Phillips Laboratory
14	Rome Laboratory
15B&15B	Wright Laboratory
16	Arnold Engineering Development Center

GSRP FINAL REPORT TABLE OF CONTENTS i-xi

APPENDICIES:

SRP Final Report Table of Contents

SRP Final Report Table of Contents

SRP Final Report Table of Contents

SRP Final Report Table of Contents

SRP Final Report Table of Contents

SRP Final Report Table of Contents

SRP Final Report Table of Contents

SRP Final Report Table of Contents

SRP Final Report Table of Contents

SRP Final Report Table of Contents

SRP Final Report Table of Contents

1. INTRODUCTION

The Summer Research Program (SRP), sponsored by the Air Force Office of Scientific Research (AFOSR), offers paid opportunities for university faculty, graduate students, and high school students to conduct research in U.S. Air Force research laboratories nationwide during the summer.

Introduced by AFOSR in 1978, this innovative program is based on the concept of teaming academic researchers with Air Force scientists in the same disciplines using laboratory facilities and equipment not often available at associates' institutions.

The Summer Faculty Research Program (SFRP) is open annually to approximately 150 faculty members with at least two years of teaching and/or research experience in accredited U.S. colleges, universities, or technical institutions. SFRP associates must be either U.S. citizens or permanent residents.

The Graduate Student Research Program (GSRP) is open annually to approximately 100 graduate students holding a bachelor's or a master's degree; GSRP associates must be U.S. citizens enrolled full time at an accredited institution.

The High School Apprentice Program (HSAP) annually selects about 125 high school students located within a twenty mile commuting distance of participating Air Force laboratories.

AFOSR also offers its research associates an opportunity, under the Summer Research Extension Program (SREP), to continue their AFOSR-sponsored research at their home institutions through the award of research grants. In 1994 the maximum amount of each grant was increased from $20,000 to $25,000, and the number of AFOSR-sponsored grants decreased from 75 to 60. A separate annual report is compiled on the SREP.

The numbers of projected summer research participants in each of the three categories and SREP "grants" are usually increased through direct sponsorship by participating laboratories.

AFOSR's SRP has well served its objectives of building critical links between Air Force research laboratories and the academic community, opening avenues of communications and forging new research relationships between Air Force and academic technical experts in areas of national interest, and strengthening the nation's efforts to sustain careers in science and engineering. The success of the SRP can be gauged from its growth from inception (see Table 1) and from the favorable responses the 1997 participants expressed in end-of-tour SRP evaluations (Appendix B).

AFOSR contracts for administration of the SRP by civilian contractors. The contract was first awarded to Research & Development Laboratories (RDL) in September 1990. After completion of the

1990 contract, RDL (in 1993) won the recompetition for the basic year and four 1-year options.

2. PARTICIPATION IN THE SUMMER RESEARCH PROGRAM

The SRP began with faculty associates in 1979; graduate students were added in 1982 and high school students in 1986. The following table shows the number of associates in the program each year.

YEAR	SRP Participation, by Year			TOTAL
	SFRP	GSRP	HSAP	
1979	70			70
1980	87			87
1981	87			87
1982	91	17		108
1983	101	53		154
1984	152	84		236
1985	154	92		246
1986	158	100	42	300
1987	159	101	73	333
1988	153	107	101	361
1989	168	102	103	373
1990	165	121	132	418
1991	170	142	132	444
1992	185	121	159	464
1993	187	117	136	440
1994	192	117	133	442
1995	190	115	137	442
1996	188	109	138	435
1997	148	98	140	427

Beginning in 1993, due to budget cuts, some of the laboratories weren't able to afford to fund as many associates as in previous years. Since then, the number of funded positions has remained fairly constant at a slightly lower level.

3. RECRUITING AND SELECTION

The SRP is conducted on a nationally advertised and competitive-selection basis. The advertising for faculty and graduate students consisted primarily of the mailing of 8,000 52-page SRP brochures to chairpersons of departments relevant to AFOSR research and to administrators of grants in accredited universities, colleges, and technical institutions. Historically Black Colleges and Universities (HBCUs) and Minority Institutions (MIs) were included. Brochures also went to all participating USAF laboratories, the previous year's participants, and numerous individual requesters (over 1000 annually).

RDL placed advertisements in the following publications: *Black Issues in Higher Education, Winds of Change,* and *IEEE Spectrum.* Because no participants list either *Physics Today* or *Chemical & Engineering News* as being their source of learning about the program for the past several years, advertisements in these magazines were dropped, and the funds were used to cover increases in brochure printing costs.

High school applicants can participate only in laboratories located no more than 20 miles from their residence. Tailored brochures on the HSAP were sent to the head counselors of 180 high schools in the vicinity of participating laboratories, with instructions for publicizing the program in their schools. High school students selected to serve at Wright Laboratory's Armament Directorate (Eglin Air Force Base, Florida) serve eleven weeks as opposed to the eight weeks normally worked by high school students at all other participating laboratories.

Each SFRP or GSRP applicant is given a first, second, and third choice of laboratory. High school students who have more than one laboratory or directorate near their homes are also given first, second, and third choices.

Laboratories make their selections and prioritize their nominees. AFOSR then determines the number to be funded at each laboratory and approves laboratories' selections.

Subsequently, laboratories use their own funds to sponsor additional candidates. Some selectees do not accept the appointment, so alternate candidates are chosen. This multi-step selection procedure results in some candidates being notified of their acceptance after scheduled deadlines. The total applicants and participants for 1997 are shown in this table.

1997 Applicants and Participants			
PARTICIPANT CATEGORY	TOTAL APPLICANTS	SELECTEES	DECLINING SELECTEES
SFRP	490	188	32
(HBCU/MI)	(0)	(0)	(0)
GSRP	202	98	9
(HBCU/MI)	(0)	(0)	(0)
HSAP	433	140	14
TOTAL	1125	426	55

4. SITE VISITS

During June and July of 1997, representatives of both AFOSR/NI and RDL visited each participating laboratory to provide briefings, answer questions, and resolve problems for both laboratory personnel and participants. The objective was to ensure that the SRP would be as constructive as possible for all participants. Both SRP participants and RDL representatives found these visits beneficial. At many of the laboratories, this was the only opportunity for all participants to meet at one time to share their experiences and exchange ideas.

5. HISTORICALLY BLACK COLLEGES AND UNIVERSITIES AND MINORITY INSTITUTIONS (HBCU/MIs)

Before 1993, an RDL program representative visited from seven to ten different HBCU/MIs annually to promote interest in the SRP among the faculty and graduate students. These efforts were marginally effective, yielding a doubling of HBCI/MI applicants. In an effort to achieve AFOSR's goal of 10% of all applicants and selectees being HBCU/MI qualified, the RDL team decided to try other avenues of approach to increase the number of qualified applicants. Through the combined efforts of the AFOSR Program Office at Bolling AFB and RDL, two very active minority groups were found, HACU (Hispanic American Colleges and Universities) and AISES (American Indian Science and Engineering Society). RDL is in communication with representatives of each of these organizations on a monthly basis to keep up with the their activities and special events. Both organizations have widely-distributed magazines/quarterlies in which RDL placed ads.

Since 1994 the number of both SFRP and GSRP HBCU/MI applicants and participants has increased ten-fold, from about two dozen SFRP applicants and a half dozen selectees to over 100 applicants and two dozen selectees, and a half-dozen GSRP applicants and two or three selectees to 18 applicants and 7 or 8 selectees. Since 1993, the SFRP had a two-fold applicant increase and a two-fold selectee increase. Since 1993, the GSRP had a three-fold applicant increase and a three to four-fold increase in selectees.

In addition to RDL's special recruiting efforts, AFOSR attempts each year to obtain additional funding or use leftover funding from cancellations the past year to fund HBCU/MI associates. This year, 5 HBCU/MI SFRPs declined after they were selected (and there was no one qualified to replace them with). The following table records HBCU/MI participation in this program.

SRP HBCU/MI Participation, By Year				
YEAR	SFRP		GSRP	
	Applicants	Participants	Applicants	Participants
1985	76	23	15	11
1986	70	18	20	10
1987	82	32	32	10
1988	53	17	23	14
1989	39	15	13	4
1990	43	14	17	3
1991	42	13	8	5
1992	70	13	9	5
1993	60	13	6	2
1994	90	16	11	6
1995	90	21	20	8
1996	119	27	18	7

6. SRP FUNDING SOURCES

Funding sources for the 1997 SRP were the AFOSR-provided slots for the basic contract and laboratory funds. Funding sources by category for the 1997 SRP selected participants are shown here.

1997 SRP FUNDING CATEGORY	SFRP	GSRP	HSAP
AFOSR Basic Allocation Funds	141	89	123
USAF Laboratory Funds	48	9	17
HBCU/MI By AFOSR (Using Procured Addn'l Funds)	0	0	N/A
TOTAL	9	98	140

SFRP - 188 were selected, but thirty two canceled too late to be replaced.
GSRP - 98 were selected, but nine canceled too late to be replaced.
HSAP - 140 were selected, but fourteen canceled too late to be replaced.

7. COMPENSATION FOR PARTICIPANTS

Compensation for SRP participants, per five-day work week, is shown in this table.

1997 SRP Associate Compensation

PARTICIPANT CATEGORY	1991	1992	1993	1994	1995	1996	1997
Faculty Members	$690	$718	$740	$740	$740	$770	$770
Graduate Student (Master's Degree)	$425	$442	$455	$455	$455	$470	$470
Graduate Student (Bachelor's Degree)	$365	$380	$391	$391	$391	$400	$400
High School Student (First Year)	$200	$200	$200	$200	$200	$200	$200
High School Student (Subsequent Years)	$240	$240	$240	$240	$240	$240	$240

The program also offered associates whose homes were more than 50 miles from the laboratory an expense allowance (seven days per week) of $50/day for faculty and $40/day for graduate students. Transportation to the laboratory at the beginning of their tour and back to their home destinations at the end was also reimbursed for these participants. Of the combined SFRP and GSRP associates, 65 % (194 out of 286) claimed travel reimbursements at an average round-trip cost of $776.

Faculty members were encouraged to visit their laboratories before their summer tour began. All costs of these orientation visits were reimbursed. Forty-three percent (85 out of 188) of faculty associates took orientation trips at an average cost of $388. By contrast, in 1993, 58 % of SFRP associates took orientation visits at an average cost of $685; that was the highest percentage of associates opting to take an orientation trip since RDL has administered the SRP, and the highest average cost of an orientation trip. These 1993 numbers are included to show the fluctuation which can occur in these numbers for planning purposes.

Program participants submitted biweekly vouchers countersigned by their laboratory research focal point, and RDL issued paychecks so as to arrive in associates' hands two weeks later.

This is the second year of using direct deposit for the SFRP and GSRP associates. The process went much more smoothly with respect to obtaining required information from the associates, only 7% of the associates' information needed clarification in order for direct deposit to properly function as opposed to 10% from last year. The remaining associates received their stipend and expense payments via checks sent in the US mail.

HSAP program participants were considered actual RDL employees, and their respective state and federal income tax and Social Security were withheld from their paychecks. By the nature of their independent research, SFRP and GSRP program participants were considered to be consultants or independent contractors. As such, SFRP and GSRP associates were responsible for their own income taxes, Social Security, and insurance.

8. CONTENTS OF THE 1997 REPORT

The complete set of reports for the 1997 SRP includes this program management report (Volume 1) augmented by fifteen volumes of final research reports by the 1997 associates, as indicated below:

1997 SRP Final Report Volume Assignments

LABORATORY	SFRP	GSRP	HSAP
Armstrong	2	7	12
Phillips	3	8	13
Rome	4	9	14
Wright	5A, 5B	10	15
AEDC, ALCs, WHMC	6	11	16

APPENDIX A – PROGRAM STATISTICAL SUMMARY

A. Colleges/Universities Represented

Selected SFRP associates represented 169 different colleges, universities, and institutions, GSRP associates represented 95 different colleges, universities, and institutions.

B. States Represented

SFRP -Applicants came from 47 states plus Washington D.C. Selectees represent 44 states.

GSRP - Applicants came from 44 states. Selectees represent 32 states.

HSAP - Applicants came from thirteen states. Selectees represent nine states.

Total Number of Participants	
SFRP	189
GSRP	97
HSAP	140
TOTAL	426

Degrees Represented			
	SFRP	GSRP	TOTAL
Doctoral	184	0	184
Master's	2	41	43
Bachelor's	0	56	56
TOTAL	186	97	298

SFRP Academic Titles	
Assistant Professor	64
Associate Professor	70
Professor	40
Instructor	0
Chairman	1
Visiting Professor	1
Visiting Assoc. Prof.	1
Research Associate	9
TOTAL	186

Source of Learning About the SRP		
Category	Applicants	Selectees
Applied/participated in prior years	28%	34%
Colleague familiar with SRP	19%	16%
Brochure mailed to institution	23%	17%
Contact with Air Force laboratory	17%	23%
IEEE Spectrum	2%	1%
BIIHE	1%	1%
Other source	10%	8%
TOTAL	100%	100%

APPENDIX B – SRP EVALUATION RESPONSES

1. OVERVIEW

Evaluations were completed and returned to RDL by four groups at the completion of the SRP. The number of respondents in each group is shown below.

Table B-1. Total SRP Evaluations Received

Evaluation Group	Responses
SFRP & GSRPs	275
HSAPs	113
USAF Laboratory Focal Points	84
USAF Laboratory HSAP Mentors	6

All groups indicate unanimous enthusiasm for the SRP experience.

The summarized recommendations for program improvement from both associates and laboratory personnel are listed below:

A. Better preparation on the labs' part prior to associates' arrival (i.e., office space, computer assets, clearly defined scope of work).

B. Faculty Associates suggest higher stipends for SFRP associates.

C. Both HSAP Air Force laboratory mentors and associates would like the summer tour extended from the current 8 weeks to either 10 or 11 weeks; the groups state it takes 4-6 weeks just to get high school students up-to-speed on what's going on at laboratory. (Note: this same argument was used to raise the faculty and graduate student participation time a few years ago.)

2. 1997 USAF LABORATORY FOCAL POINT (LFP) EVALUATION RESPONSES

The summarized results listed below are from the 84 LFP evaluations received.

1. LFP evaluations received and associate preferences:

Table B-2. Air Force LFP Evaluation Responses (By Type)

		How Many Associates Would You Prefer To Get ?								(% Response)			
		SFRP				GSRP (w/Univ Professor)				GSRP (w/o Univ Professor)			
Lab	Evals Recv'd	0	1	2	3+	0	1	2	3+	0	1	2	3+
AEDC	0	-	-	-	-	-	-	-	-	-	-	-	-
WHMC	0	-	-	-	-	-	-	-	-	-	-	-	-
AL	7	28	28	28	14	54	14	28	0	86	0	14	0
USAFA	1	0	100	0	0	100	0	0	0	0	100	0	0
PL	25	40	40	16	4	88	12	0	0	84	12	4	0
RL	5	60	40	0	0	80	10	0	0	100	0	0	0
WL	46	30	43	20	6	78	17	4	0	93	4	2	0
Total	84	32%	50%	13%	5%	80%	11%	6%	0%	73%	23%	4%	0%

LFP Evaluation Summary. The summarized responses, by laboratory, are listed on the following page. LFPs were asked to rate the following questions on a scale from 1 (below average) to 5 (above average).

2. LFPs involved in SRP associate application evaluation process:
    a. Time available for evaluation of applications:
    b. Adequacy of applications for selection process:
3. Value of orientation trips:
4. Length of research tour:
5. a. Benefits of associate's work to laboratory:
    b. Benefits of associate's work to Air Force:
6. a. Enhancement of research qualifications for LFP and staff:
    b. Enhancement of research qualifications for SFRP associate:
    c. Enhancement of research qualifications for GSRP associate:
7. a. Enhancement of knowledge for LFP and staff:
    b. Enhancement of knowledge for SFRP associate:
    c. Enhancement of knowledge for GSRP associate:
8. Value of Air Force and university links:
9. Potential for future collaboration:
10. a. Your working relationship with SFRP:
    b. Your working relationship with GSRP:
11. Expenditure of your time worthwhile:

(Continued on next page)

12. Quality of program literature for associate:
13. a. Quality of RDL's communications with you:
    b. Quality of RDL's communications with associates:
14. Overall assessment of SRP:

Table B-3. Laboratory Focal Point Reponses to above questions

	AEDC	*AL*	*USAFA*	*PL*	*RL*	*WHMC*	*WL*
# Evals Recv'd	0	7	1	14	5	0	46
Question #							
2	-	86 %	0 %	88 %	80 %	-	85 %
2a	-	4.3	n/a	3.8	4.0	-	3.6
2b	-	4.0	n/a	3.9	4.5	-	4.1
3	-	4.5	n/a	4.3	4.3	-	3.7
4	-	4.1	4.0	4.1	4.2	-	3.9
5a	-	4.3	5.0	4.3	4.6	-	4.4
5b	-	4.5	n/a	4.2	4.6	-	4.3
6a	-	4.5	5.0	4.0	4.4	-	4.3
6b	-	4.3	n/a	4.1	5.0	-	4.4
6c	-	3.7	5.0	3.5	5.0	-	4.3
7a	-	4.7	5.0	4.0	4.4	-	4.3
7b	-	4.3	n/a	4.2	5.0	-	4.4
7c	-	4.0	5.0	3.9	5.0	-	4.3
8	-	4.6	4.0	4.5	4.6	-	4.3
9	-	4.9	5.0	4.4	4.8	-	4.2
10a	-	5.0	n/a	4.6	4.6	-	4.6
10b	-	4.7	5.0	3.9	5.0	-	4.4
11	-	4.6	5.0	4.4	4.8	-	4.4
12	-	4.0	4.0	4.0	4.2	-	3.8
13a	-	3.2	4.0	3.5	3.8	-	3.4
13b	-	3.4	4.0	3.6	4.5	-	3.6
14	-	4.4	5.0	4.4	4.8	-	4.4

3. 1997 SFRP & GSRP EVALUATION RESPONSES

The summarized results listed below are from the 257 SFRP/GSRP evaluations received.

Associates were asked to rate the following questions on a scale from 1 (below average) to 5 (above average) - by Air Force base results and over-all results of the 1997 evaluations are listed after the questions.

1. The match between the laboratories research and your field:
2. Your working relationship with your LFP:
3. Enhancement of your academic qualifications:
4. Enhancement of your research qualifications:
5. Lab readiness for you: LFP, task, plan:
6. Lab readiness for you: equipment, supplies, facilities:
7. Lab resources:
8. Lab research and administrative support:
9. Adequacy of brochure and associate handbook:
10. RDL communications with you:
11. Overall payment procedures:
12. Overall assessment of the SRP:
13.
    a. Would you apply again?
    b. Will you continue this or related research?
14. Was length of your tour satisfactory?
15. Percentage of associates who experienced difficulties in finding housing:
16. Where did you stay during your SRP tour?
    a. At Home:
    b. With Friend:
    c. On Local Economy:
    d. Base Quarters:
17. Value of orientation visit:
    a. Essential:
    b. Convenient:
    c. Not Worth Cost:
    d. Not Used:

SFRP and GSRP associate's responses are listed in tabular format on the following page.

Table B-4. 1997 SFRP & GSRP Associate Responses to SRP Evaluation

	Arnold	Brooks	Edwards	Eglin	Griffis	Hanscom	Kelly	Kirtland	Lackland	Robins	Tyndall	WPAFB	average
# res	6	48	6	14	31	19	3	32	1	2	10	85	257
1	4.8	4.4	4.6	4.7	4.4	4.9	4.6	4.6	5.0	5.0	4.0	4.7	4.6
2	5.0	4.6	4.1	4.9	4.7	4.7	5.0	4.7	5.0	5.0	4.6	4.8	4.7
3	4.5	4.4	4.0	4.6	4.3	4.2	4.3	4.4	5.0	5.0	4.5	4.3	4.4
4	4.3	4.5	3.8	4.6	4.4	4.4	4.3	4.6	5.0	4.0	4.4	4.5	4.5
5	4.5	4.3	3.3	4.8	4.4	4.5	4.3	4.2	5.0	5.0	3.9	4.4	4.4
6	4.3	4.3	3.7	4.7	4.4	4.5	4.0	3.8	5.0	5.0	3.8	4.2	4.2
7	4.5	4.4	4.2	4.8	4.5	4.3	4.3	4.1	5.0	5.0	4.3	4.3	4.4
8	4.5	4.6	3.0	4.9	4.4	4.3	4.3	4.5	5.0	5.0	4.7	4.5	4.5
9	4.7	4.5	4.7	4.5	4.3	4.5	4.7	4.3	5.0	5.0	4.1	4.5	4.5
10	4.2	4.4	4.7	4.4	4.1	4.1	4.0	4.2	5.0	4.5	3.6	4.4	4.3
11	3.8	4.1	4.5	4.0	3.9	4.1	4.0	4.0	3.0	4.0	3.7	4.0	4.0
12	5.7	4.7	4.3	4.9	4.5	4.9	4.7	4.6	5.0	4.5	4.6	4.5	4.6
Numbers below are percentages													
13a	83	90	83	93	87	75	100	81	100	100	100	86	87
13b	100	89	83	100	94	98	100	94	100	100	100	94	93
14	83	96	100	90	87	80	100	92	100	100	70	84	88
15	17	6	0	33	20	76	33	25	0	100	20	8	39
16a	-	26	17	9	38	23	33	4	-	-	-	30	
16b	100	33	-	40	-	8	-	-	-	-	36	2	
16c	-	41	83	40	62	69	67	96	100	100	64	68	
16d	-	-	-	-	-	-	-	-	-	-	-	0	
17a	-	33	100	17	50	14	67	39	-	50	40	31	35
17b	-	21	-	17	10	14	-	24	-	50	20	16	16
17c	-	-	-	-	10	7	-	-	-	-	-	2	3
17d	100	46	-	66	30	69	33	37	100	-	40	51	46

4. 1997 USAF LABORATORY HSAP MENTOR EVALUATION RESPONSES

Not enough evaluations received (5 total) from Mentors to do useful summary.

5. 1997 HSAP EVALUATION RESPONSES

The summarized results listed below are from the 113 HSAP evaluations received.

HSAP apprentices were asked to rate the following questions on a scale from
1 (below average) to 5 (above average)

1. Your influence on selection of topic/type of work.
2. Working relationship with mentor, other lab scientists.
3. Enhancement of your academic qualifications.
4. Technically challenging work.
5. Lab readiness for you: mentor, task, work plan, equipment.
6. Influence on your career.
7. Increased interest in math/science.
8. Lab research & administrative support.
9. Adequacy of RDL's Apprentice Handbook and administrative materials.
10. Responsiveness of RDL communications.
11. Overall payment procedures.
12. Overall assessment of SRP value to you.
13. Would you apply again next year? Yes (92 %)
14. Will you pursue future studies related to this research? Yes (68 %)
15. Was Tour length satisfactory? Yes (82 %)

	Arnold	Brooks	Edwards	Eglin	Griffiss	Hanscom	Kirtland	Tyndall	WPAFB	Totals
# resp	5	19	7	15	13	2	7	5	40	113
1	2.8	3.3	3.4	3.5	3.4	4.0	3.2	3.6	3.6	3.4
2	4.4	4.6	4.5	4.8	4.6	4.0	4.4	4.0	4.6	4.6
3	4.0	4.2	4.1	4.3	4.5	5.0	4.3	4.6	4.4	4.4
4	3.6	3.9	4.0	4.5	4.2	5.0	4.6	3.8	4.3	4.2
5	4.4	4.1	3.7	4.5	4.1	3.0	3.9	3.6	3.9	4.0
6	3.2	3.6	3.6	4.1	3.8	5.0	3.3	3.8	3.6	3.7
7	2.8	4.1	4.0	3.9	3.9	5.0	3.6	4.0	4.0	3.9
8	3.8	4.1	4.0	4.3	4.0	4.0	4.3	3.8	4.3	4.2
9	4.4	3.6	4.1	4.1	3.5	4.0	3.9	4.0	3.7	3.8
10	4.0	3.8	4.1	3.7	4.1	4.0	3.9	2.4	3.8	3.8
11	4.2	4.2	3.7	3.9	3.8	3.0	3.7	2.6	3.7	3.8
12	4.0	4.5	4.9	4.6	4.6	5.0	4.6	4.2	4.3	4.5
Numbers below are percentages										
13	60%	95%	100%	100%	85%	100%	100%	100%	90%	92%
14	20%	80%	71%	80%	54%	100%	71%	80%	65%	68%
15	100%	70%	71%	100%	100%	50%	86%	60%	80%	82%

INCORPORATING CONDENSATION INTO NASTD

Jessica L. Thomas
Graduate Research Assistant
Department of Mathematics

University of Tennessee Space Institute
B. H. Goethert Pkwy
Tullahoma, TN 37388

Final Report for:
Graduate Student Research Program
Arnold Engineering Development Center

Sponsored by:
Air Force Office of Scientific Research
Boling Air Force Base, DC

and

Arnold Engineering Development Center

September 1997

INCORPORATING CONDENSATION INTO NASTD

Jessica L. Thomas
Graduate Research Assistant
Department of Mathematics
University of Tennessee Space Institute

Abstract

The goal of this study is to inexpensively obtain flow conditions which ideally are suited for flow visualization techniques involving vapor screens by incorporating condensation routines into the McDonnell Douglas NASTD code. The analysis follows that by Ryzhov, Pirumov, and Gorbunov and results in the Fokker-Planck equation which must be solved numerically by iteration. Further work will involve writing appropriate subroutines to perform this task and incorporating them into NASTD which will then be used to calculate the optimal flow conditions for flow visualization.

INCORPORATING CONDENSATION INTO NASTD

Jessica L. Thomas

Introduction

A popular method of flow visualization in wind tunnel testing involves vapor screens which rely on the presence of water droplets in the flow field of interest. Before running an expensive test the scientist would like to have a good idea of the initial conditions required to produce the desired droplet size and distribution during the actual test. To obtain these conditions quickly and inexpensively CFD codes with condensation capability can be used {1}. The overall purpose of this study is to improve the McDonnell Douglas NASTD code be incorporating routines to calculate condensation in the computational domain. To assist in the development a flow chart was made listing all subroutines called within the code. Then a literature search was performed to obtain a better idea of the physical laws governing condensation.

Methodology and Results

In this study the analysis follows that given in {2}. Interest is placed on spherical liquid droplets in a vapor medium with the assumption of equilibrium between the droplet and surrounding vapor. Also, the liquid and gaseous phases have the same temperature. To describe the nucleation of these spherical droplets, the change in the Gibbs free energy is used:

$$\Delta G = g[\mu_l(p_\infty,T) - \mu_v(p_v,T)] + 4\pi r^2\sigma \tag{1}$$

where g is the number of molecules in a droplet with radius r, μ_l and μ_v are the chemical potentials of the liquid and the vapor, p_v and p_∞ are the vapor pressure and saturation vapor pressure, and σ is the specific surface free energy (surface tension). The radius can be written as:

$$r = \left(\frac{3gV_l}{4\pi}\right)^{1/3} \tag{2}$$

where V_l is the volume per molecule. It is obvious from (2) that:

$$g = 4\pi r^3 V_l \tag{3}$$

To determine the equilibrium conditions, ΔG is minimized:

$$\frac{d\Delta G}{dg} = \mu_l(p_\infty,T) - \mu_v(p_v,T) + 4\pi\sigma\frac{dr^2}{dg}\left(1+\frac{1}{2}\frac{d\ln\sigma}{dr^2}\right) = 0 \tag{4}$$

The critical radius r^* can be acquired from (4) if σ is not dependent on r:

$$r^* = \frac{2\sigma V_l}{\mu_v(p_v,T) - \mu_l(p_\infty,T)} \tag{5}$$

For an ideal gas $\mu_v(p_v,T) - \mu_l(p_\infty,T) = kT\ln(p_v/p_\infty)$ and so (5) is:

$$r^* = \frac{2\sigma V_l}{kT\ln\left(\frac{p_v}{p_\infty}\right)} \quad \text{or} \quad \ln\left(\frac{p_v}{p_\infty}\right) = \left(\frac{2\sigma V_l}{r^*kT}\right) \tag{6}$$

By substitution the number of molecules in a droplet at r^* becomes:

$$g^* = \frac{8}{3}\pi\frac{\sigma r^{*2}}{\mu_v(p_v,T) - \mu_l(p_\infty,T)} \tag{7}$$

and also:

$$\Delta G^* = \frac{16\pi}{3}\left(\frac{V_l}{\mu_v(p_v,T) - \mu_l(p_\infty,T)}\right)^2\sigma^3 \tag{8}$$

Using (5)-(7) and (1) ΔG can be expressed as:

$$\Delta G = \sigma\left(\frac{4\pi V_l^2}{3}\right)^{1/3} g^{*2/3}\left[3\left(\frac{g}{g^*}\right)^{2/3} - 2\frac{g}{g^*}\right] \tag{9}$$

Nucleation occurs when the clusters of molecules in a vapor combine with another molecule which results in larger clusters. To show this process for the addition of a single vapor molecule A_1, consider:

$$A_1 + A_1 \Leftrightarrow A_2$$
$$A_2 + A_1 \Leftrightarrow A_3$$
$$\vdots$$
$$A_{G-1} + A_1 \Leftrightarrow A_G$$

where $G > g^*$ and A_i is a cluster with g molecules (g-mers). In the case of condensation, clusters grow from A_i to A_{i+1} by the addition of a single molecule; conversely, evaporation results from the loss of a molecule (i.e. A_{i+1} to

A_i) where the cluster becomes smaller. Also, the formation of larger clusters can result from the collision of two smaller clusters:

$$A_i + A_j \rightarrow A_{i+j}$$

or can separate into two smaller clusters:

$$A_{i+j} \rightarrow A_i + A_j$$

However, except for the case of formation of dimers:

$$A_1 + A_1 + A_1 \Leftrightarrow A_2 + A_1; A_1 + A_1 + B \Leftrightarrow A_2 + B$$

where B is a third substance such as the carrier gas, these reactions have little affect on condensation. Condensation occurs when the growth process dominates the decay process and the number of large clusters increases. The rate of formation of clusters containing g molecules I_g can be found if the reaction rate constants are known. The forward reaction constant is given by:

$$K_g^{(f)} = \alpha_c 4\pi r^2 \frac{p_v}{(2\pi mkT)^{1/2}} \tag{10}$$

where α_c is the condensation coefficient. Since the reverse reaction constant $K_g^{(r)}$ is difficult to determine the ratio of the reaction rates is:

$$K_g = \frac{n_g}{n_{g-1} n_1} = \frac{K_g^{(f)}}{K_g^{(r)}} \tag{11}$$

where

$$n_g = n_1 exp\left(-\frac{\Delta G}{kT}\right) \tag{12}$$

From the evaporation and condensation reactions, the number of clusters of class g per unit volume f_g can be obtained by the following equation:

$$\frac{\partial f_g}{\partial t} = I_g - I_{g+1}, g = (2, \ldots, G) \tag{13}$$

where from (11)

$$I_g = K_g^{(f)} n_1 f_{g-1} - K_g^{(r)} f_g = K_g^{(f)} n_1 n_{g-1} \left(\frac{f_{g-1}}{n_{g-1}} - \frac{f_g}{n_g} \right) \tag{14}$$

For equilibrium conditions the number of clusters is given by n_g and can be found from (12), but for the nonequilibrium conditions the system of differential equations (13) must be solved to find f_g. For very large g, where $\Delta g = \pm 1$ (14) can be rewritten as:

$$I(g,t) = -K_g^{(f)} n_1 n_g \frac{\partial}{\partial g} \left(\frac{f_g}{n_g} \right) = -D \frac{\partial f}{\partial g} - \frac{Df}{kT} \frac{\partial \Delta G}{\partial g} \tag{15}$$

where $D = K_g^{(f)} n_1$ and $\Delta g = dg$. Another substitution of $\partial I / \partial g$ for $I_g - I_{g+1}$ in equation (13) gives:

$$\frac{\partial f}{\partial t} = -\frac{\partial I}{\partial g} = \frac{\partial}{\partial g} \left(D \frac{\partial f}{\partial g} \right) + \frac{1}{kT} \frac{\partial}{\partial g} \left(Df \frac{\partial \Delta G}{\partial g} \right) \tag{16}$$

This Fokker-Planck equation in future study is to be solved numerically for f_g.

References

1. F. G. Collins, "Development of Laser Vapor Screen Flow Visualization System for 16T," AEDC-TMR-96-E8, September, 1996.

2. Y. A. Ryzhov, U. G. Pirumov, and V. N. Gorbunov, Nonequilibrium Condensation in High-Speed Gas Flows, Gordon and Breach, New York, 1989.

HUE ANALYSIS FACTORS FOR LIQUID CRYSTAL TRANSIENT HEAT TRANSFER MEASUREMENTS

Derek E. Lang
Graduate Student
Department of Aeronautics

University of Washington
Guggenheim Building
Seattle, WA 98195

Final Report for:
Graduate Student Research Program
U.S. Air Force Academy/Aeronautics Research Center

Sponsored by:
Air Force Office of Scientific Research
Bolling Air Force Base, DC

And

U.S. Air Force Academy/Aeronautics Research Center

September 1997

HUE ANALYSIS FACTORS FOR LIQUID CRYSTAL TRANSIENT HEAT TRANSFER MEASUREMENTS

Derek E. Lang
Graduate Student
Department of Aeronautics
University of Washington

Abstract

Hue Analysis is one approach for using liquid crystals to measure transient heat transfer in high speed flows. The indications given by wide-band crystals that are used to determine temperature, however, are highly sensitive to flow conditions, model material properties, viewing angles and illumination, and framegrabbing rate. This study used the hue capture range and duration of crystal colorplay as a measure the significance and influence of these factors in providing sufficient information to accurately measure temperature changes. An Experimental Design approach was used to define the test strategies and analyze the data. It was found that materials with high $(\rho ck)^{1/2}$, $k/\rho c$, and wide bandwidth crystals are the most critical factors. The hue analysis was then applied to various model geometries to illustrate the use of liquid crystals to measure heat transfer, and identify various boundary layer features.

HUE ANALYSIS FACTORS FOR LIQUID CRYSTAL TRANSIENT HEAT TRANSFER MEASUREMENTS

Derek E. Lang

Introduction

The U.S. Air Force Academy/Aeronautical Research Center (ARC) is developing the capability to measure heat transfer in its Trisonic Wind Tunnel (TWT). One measurement technique assessed by ARC is liquid crystal thermography. This technique can be used to provide information about the global heat transfer on the surface of a the desired geometry. Thermochromic liquid crystals are surface coatings that change color with temperature. The monitoring of these temperature changes on a model surface with time are directly related to the heat transfer. Heat transfer measurements by liquid crystals are sensitive to a number of factors, ranging from the selection of the crystal and model materials to the application of the crystals and test conditions. This research analyzes the effect of these factors on liquid crystal measurements in the TWT test environments at ARC.

Methodology

The rate of heat transfer is dependent on the characteristics of the boundary layer formed at the model surface and the temperature differences driving the heat transfer. The heat flux equation below illustrates the dependence on the heat transfer coefficient, h, the adiabatic wall temperature, T_{aw}, and the wall temperature, T_w.

$$q = h\,(T_{aw} - T_w)$$

The experimentalist determines heat transfer by measuring surface temperature(s) at given locations over time. Lang (Ref. 1) describes several methods for reducing this temperature data to heat transfer.

Ireland et. al. (Ref. 2) describe the liquid crystal measurement techniques used to accurately provide a single temperature measurement or continuous temperature data depending on the data reduction method used. In hue analysis, the hue of the liquid crystal is correlated with specific temperatures. Hue is one component along with saturation and value (or intensity) used to define liquid crystal color. The crystal temperature bandwidth is selected so that colorplay (i.e., hue changes in this case) occurs for the temperatures of interest. For example, a crystal bandwidth spanning the temperature range of the model surface during the test provides continuous information about the flow over the surface.

Table 1 lists several factors contributing to the accuracy, or conversely uncertainty, of the heat transfer rate computed. This study focuses on those factors affecting the ability to measure temperature using liquid crystals. Experiments with liquid crystals on models in the TWT were conducted to evaluate effects of the models' geometry and material properties (thermal conductivity, k, density, ρ, and specific heat, c_p), crystal bandwidth and total temperature. Model geometry effects are also related to heat-transfer rates, viewing angles, and illumination.

Initially, the hues for the Hallcrest BM/R12C6W/C17-10 crystal with 6°C bandwidth and BM/12RC2W/17-10 crystal with 2°C bandwidth were correlated to temperatures in a static calibration rig. The Image Therm Engineering Liquid Crystal-Temperature Response Calibration Unit, MK II, insulated the liquid crystal which was sprayed onto a copper substrate and created a temperature gradient along the substrate length. Type-K thermocouples measured temperature at uniform distances along the substrate. The calibration rig was place inside the Trisonic Wind Tunnel to represent an in-situ environment. Florescent lights placed at 45-degree angles above and below the viewing window illuminated the substrate inside the tunnel. A Sony 3ccd Color Vision Camera (with RGB format) monitored the crystals at 30 Hz. A Matrox Meteor framegrabber captured the images at a user-defined rate and saved them on a personal computer.

Several models with a liquid crystal were then tested in the TWT with the test configurations in Table 2 to screen for significant factors under supersonic flow conditions. The TWT is a supersonic blowdown facility capable of producing up to Mach 4.28 flows. The TWT was operated at total temperatures of 22-35°C with a stilling chamber pressure of 1.2×10^6 N/m^2. The model surface temperature decreased to temperatures of -5°C once supersonic flow was established. Figure 1 shows the models used to represent the different heat transfer characteristics that ARC may investigate, including: sharp and blunted cones, a missile, a lifting body, and airframe-propulsion integrated vehicle forebody (i.e., API model). Table 3 lists the model materials and properties. Omega "Cement-On" type-E thermocouples were attached to the model surfaces to verify temperature readings. The liquid crystal was applied using airbrush with a minimum number of passes over the surfaces to ensure a thin coating.

The measures of these factors' influences were hue range captured by the video framegrabber as temperatures pass through the crystal bandwidth and the duration of this colorplay. Hue range is the usable portion of the hue spectrum that can be correlated to a temperature. Hue range also indicates the accuracy of the temperature measurement. Duration of colorplay relates to the amount of time available to capture the hues and the speed of framegrabbing required. The Experimental Design Method described by Smith and Launsby (Ref. 3) served as the basis for the test configurations selected and data analysis.

Results

Static Calibration. Figures 2a and 2b present the calibration curves for the 6°C and 2°C crystals. The lower end of the hue scale from 0-0.17 corresponds to the color red. The colors then change from yellow to green and then blue at the upper end of the scale. Initially, it was difficult to obtain data in the hue range between 0.15 - 0.40 which encompasses the green, yellow, and red colors. As seen in the figures, the hues change rapidly with small increases in temperature for this portion of the hue spectrum. The calibration rig was limited in its ability to create the small temperature gradients necessary to isolate hues in this range. The colorplay from blue to red occurred within such a short distance along the length of the substrate that the framegrabber could not capture hues corresponding to the colors in between. Later, the crystals were cooled to temperatures below the crystal bandwidth at one end of the substrate and allowed to warm to ambient temperature. Colorplay was then spread across a wider portion of the substrate, and thermocouples recorded temperatures as the hue changes occurred. The temperature component of standard deviation from the best-fit curve was 0.55°C for the 6°C crystal and 0.52°C for the 2°C crystal. Because the entire hue spectrum must be spanned within the crystal bandwidth, the narrower bandwidth crystals will have a flatter temperature-hue curve. As a result, the impact of the ±0.3°C thermocouple uncertainty of due to noise results in wider variances from the calibration curve-fit given uncertainty in hue determination is constant between the 6°C and 2°C crystal. An optimum bandwidth must be selected, since the wider bandwidth actually increases the uncertainty in the hue.

The blue color is visible for several degrees above the manufacturer-specified upper temperature limit. As a result, the temperature-hue curve flattens above a hue of about 0.60, and the uncertainty in corresponding temperature increases. Visually, blue and red lead to black on either side of the crystal bandwidth. However, hue is measured on a radial scale so that reds occur at hues approximately 0-0.15, but reappear for hues from about 0.80 to 1.0. High hue values (e.g., above .85) with low temperatures were given subtracted from 1.0, so that they corresponded with reds at the lower hue spectrum. However, it was difficult to define the correct hue cut-off (i.e., reds might occur with hues at 0.75 up to 1.00); and it is probably better to ignore hue readings above those corresponding to the green or green/blue portion of the hue scale.

Wind Tunnel Tests. The hues recorded by the framegrabber and associated temperatures measured by thermocouple during wind tunnel tests are compared with the static calibration curve in Figure 2a. The hues captured on the cone and one of the missiles are nearly constant, even though the wall temperature decreases with time; resulting in a hue range less than 0.1. In contrast, the lifting body matches the static calibration and spans the entire usable hue range, as it should if surface temperature passes completely through the crystal bandwidth. Although a large hue range does not necessarily imply an accurate reading, a small hue range may be an indication of inaccurate temperature measurement along some portion of the hues captured.

Before assuming a problem with the hue capture, it must be realized that hue range may be limited because the surface temperature, as in some of the API model cases, never passed completely through the bandwidth, either because it reached adiabatic wall temperature or the heat transfer rate was so low. In most cases however, colorplay is completed by the end of the test run.

Hue range is also related to the ability to capture data points within the crystal bandwidth which is related to colorplay duration. The high heating rates, material properties, and framegrabbing speed allowed the framegrabber to collected only a few points for the cone presented in Figure 2a, and resulted in a small hue range. Figure 3 shows the cone temperature passes through the crystal bandwidth much faster than the lifting body. This colorplay duration thus is the lower threshold for the framegrabber speed. Figure 4 is the result of Analysis of Variance (ANOVA) applied to the colorplay duration, and confirms that material, heat transfer, and total temperature are the major factors (note: bandwidth has some effect due to statistical association). The framegrabbing speed was found to be relatively significant to the hue range in Figure 5, and should be explored further. Shutter speed may affect the hue accuracy, but framegrabbing speed would seem to only affect the number of data points captured.

Figure 2a shows that even with an adequate framegrabbing speed, the hue measurements are subject other factors leading to inaccuracy. The small hue ranges generally coincided with tests that had faint or "washed out" colors which could not be picked up as well with the framegrabber as shown in Figure 6. Lighting and glare problems existed for all of the tests, but were not likely the cause since the models showed very distinctive colors when viewed while warming up in the test section. Another potential cause of washout may be the camera shutter speed which should be examined further.

Figure 7 compares combinations of material $(\rho ck)^{1/2}$, bandwidth, and tank temperature (indicative of total temperature) for the Stycast lifting body and Plexiglas cones, which represent the wide span of the material properties in question (note: the $(\rho ck)^{1/2}$ of Ertalyte is actually slightly smaller than Plexiglas). Bandwidth is the most influential. Material property and its combination with bandwidth are also significant; whereas tank temperature has little effect. From the prediction equation below, the hue range is maximized for large bandwidths and high $(\rho ck)^{1/2}$:

$$\text{Hue Range} = 0.164 + 0.1(B) + 0.07(A) - 0.07(-A)(B)$$

Where $-1 \le A \le +1$, for bandwidths between 2°C and 6°C

$-1 \le B \le +1$, for $(\rho ck)^{1/2}$ between Plexiglas and Stycast

The analysis above assumed that given different model geometries were comparable, given similar heat transfer coefficients ($h>100$ W/m^2 in this case). Figure 5 compares the relative effects of $k/\rho c$ for a constant cone geometry and crystal bandwidth. The optimum setting would be either a low $k/\rho c$ with high heat transfer or high $k/\rho c$ with low heat transfer.

The color of the wide-band crystal is sensitive to viewing angle and illumination. In the tunnel, model viewing was complicated by glare and shadows on curved surfaces. In the case of the cones, the location of glare and shadows coincided with model curvature. A comparison of Ertalyte models attempted to isolate the effects of the two factors as shown in Figure 8. The analysis suggested that the best combination for maximizing hue range was a shadowed area at an angle to the line of sight. This seems counter-intuitive, and is even more suspect since the hue range on the lifting body indicated an indifference to lighting (though the Stycast material has other favorable characteristics that may outweigh the lighting issue). It does appear that the hue ranges on the Ertalyte models was limited more by heating and material considerations than by lighting issues. Lighting angle may also be the cause of the "tongue"-shaped color pattern present on the lower side of the nose region of the conical models. The reduction of the images repeatedly captures hues in this pattern. Additional testing should be conducted to ensure that this is an illumination issue and not due to asymmetric flow.

Flow Characterization. Once the appropriate selection of model geometries, materials, and test conditions are determined, liquid crystals provide substantial information about the flow over the model surface either through flow visualization or heat transfer distributions. For example, flow transition is generally indicated by a rise in heat transfer trend moving aft of the leading edge. This is readily seen by the liquid crystals on the API model where the beginning of transition is located at point of slowest color change in Figure 9, i.e., just before heat transfer increases. Figure 10 also illustrates the use of wide band liquid crystals to identify other flow features over the surface of the models, such as flow separation, transitional flow striations, and shock impingement.

Heat transfer data reduction is more complex depending on the assumptions and techniques used. Cook-Felderman or Kendall-Dixon methods are well suited for the transient conditions of the TWT. However, the impacts of the start-up temperature spike during a run must be carefully considered. Moreover, use of these methods generally requires a minimum sampling frequency of 50 Hz, which was greater than the current video-framegrabbing capability. Babinsky (Ref. 4) supplements liquid crystal measurements with thermocouple data to obtain global surface heat flux by temperature ratios. Figure 11 compares the heat transfer over the Missile model using this proportional heat transfer approach to application of complementary error function, and a narrow bandwidth, single-temperature method.

A common problem in determining the analytical solution for heat transfer is the lack of knowledge of the state of the boundary layer (i.e., laminar, turbulent, or transitional) and boundary conditions. Separation regions and shock interactions make it difficult to predict recovery temperature, and the use of total temperature as a substitute in the heat transfer equations is complicated by the low enthalpies flow regime of the TWT where, total temperature is greater than wall temperature while adiabatic wall temperature lower than wall temperature. The advantage of the multiple, or continuous, data readings from liquid crystals is the ability to implicitly determine recovery temperature.

Conclusions

The wide-band liquid crystals provide global measurements on a time-continuous basis. Materials with high $(\rho ck)^{1/2}$ and $k/\rho c$, lower heat transfer, wide crystal bandwidth, and high sampling frequency. Hue range is an indicator of the accuracy of the temperature measurement; while colorplay duration defines the minimum framegrabbing speeds required. Bandwidth and material selection are the most factors affecting these parameters. Crystal bandwidths should extend across the entire spectrum of wall temperatures anticipated during the test.

The size of the hue range required is dependent on the data reduction technique. For example, only one data point is needed for the complementary error function method. For this approach, it is more critical to correlate the duration of colorplay to the video-framegrabbing rate. If a continuous data reduction technique is used (e.g., Babinsky), then hue range is related to the required temperature range and measurement uncertainty levels. For the tests conducted, adequate heat transfer rates were obtained in the cases where the hue range was at a minimum 0.15-0.2 and colorplay lasted at least 10 seconds. Additional study is necessary to understand the influence of shutter speed, viewing angle and illumination. Once the model material and bandwidth are selected to give accurate temperature-hue relations, liquid crystal thermography provides significant data on the flow characteristics over complex configurations.

Acknowledgments

The author wishes to extend his deepest appreciation to the following members of the DFANL team without whom this project could not have been accomplished: Dr. John Bertin, Capt. Matt Zuber, Dr. Tom Yechout, Dr. James Baughn (007), Mr. Larry Lamblin, Mr. Jim Phelps, and Mr. Bobby Hatfield.

References

1. Lang, Derek E., "USAFA Trisonic Wind Tunnel Analysis for Heat Transfer Measurements," U.S. Air Force Academy/Aeronautics Laboratory, Report No. 96-02, August 1996.
2. Ireland, P.T., Wang, Z., and Jones, T.V., "Liquid Crystal Heat Transfer Measurements," Measurement Techniques, Lecture Series 1995-01, von Karman Institute for Fluid Dynamics, January 30-February 3, 1995.
3. Schmidt, Stephen R., and Launsby, Robert G., Understanding Industrial Designed Experiments, Air Academy Press, Colorado Springs, Colorado, 1992.
4. Babinsky, H., and Edwards, J.A., "Automatic Liquid Crystal Thermography for Transient Heat Transfer Measurements in Hypersonic Flow," Experiments in Fluids, Vol. 21, 1996, pp. 227-236.

Table 1: Factors Affecting Heat Transfer Measurements in Trisonic Wind Tunnel

Factor	Measurement Technique	Data Reduction	Flow Physics	Comment
Crystal Bandwidth	X			**Constrained by Available Crystals**
Crystal Temperature	X			**Constrained by Available Crystals**
Material (rho.c.k)	X			
Material (k/rho.c)	X			
Model Geometry	X	X	X	
Total Pressure			X	
Total Temperature	X	X	X	
Mach Number	X	X	X	**Focus on M = 4.28**
Coating Thickness	X	X		**Kept relatively constant; assume negligible affect on heat transfer**
Illumination	X			**Can keep constant once configured**
Viewing Angles	X			
Start Time Uncertainty		X		
Initial Surface Temperature		X		
Data Reduction Assumptions		X		**Assume h converges to constant**

Table 2: Test Configurations

Geometry	Material	Bandwidth (deg)	Tank Temp (F)
Sharp Cone	Plexiglas	2	90
Sharp Cone	Plexiglas	2	110
Sharp Cone	Plexiglas	6	90
Sharp Cone	Plexiglas	6	110
Sharp Cone	Ertalyte	6	110
Sharp Cone	Agloflon	6	110
Blunt Cone	Plexiglas	6	110
Blunt Cone	Ertalyte	6	110
Blunt Cone	Agloflon	6	90
Blunt Cone	Agloflon	6	110
Missile	Ertalyte	6	110
Lifting Body	Stycast	2	90
Lifting Body	Stycast	2	110
Lifting Body	Stycast	6	90
Lifting Body	Stycast	6	110
API	Plexiglas	6	110
API	Ertalyte	6	110

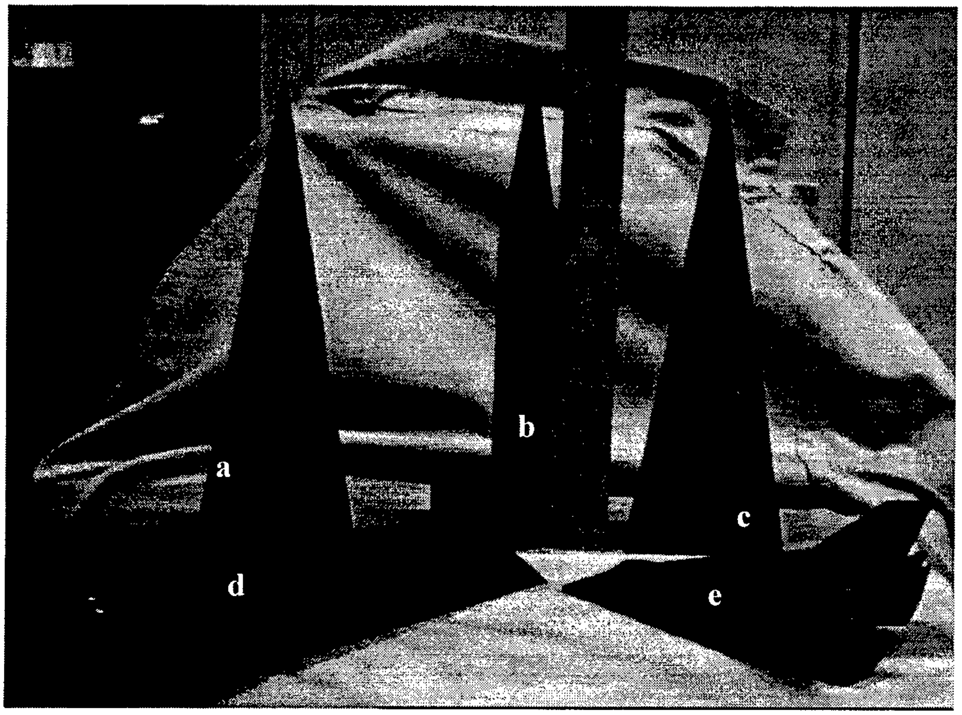

Figure 1: Models used (a) Sharp Cone; (b) Missile; (c) Slightly Blunted Cone; (d) Airframe Propulsion Integration (API); and (e) Lifting Body.

Table 3 - Model Material Properties

Material	Density (kg/m^3)	Specific Heat (J/Kg.K)	Thermal Conductivity (J/Kg.K)	sqrt(rho.c.k) ($Ws^{1/2}/m^2.K$)	k/rho.c ($1/m^2s$)
Plexiglas	**1190**	**1462**	**.19**	**575**	**6.90e-8**
Ertalyte	**1201**	**1075**	**1.26**	**501**	**1.50e-7**
Agloflon	**2220**	**981**	**.34**	**861**	**1.56e-7**
Stycast	**2277**	**904**	**1.24**	**1594**	**6.03e-7**

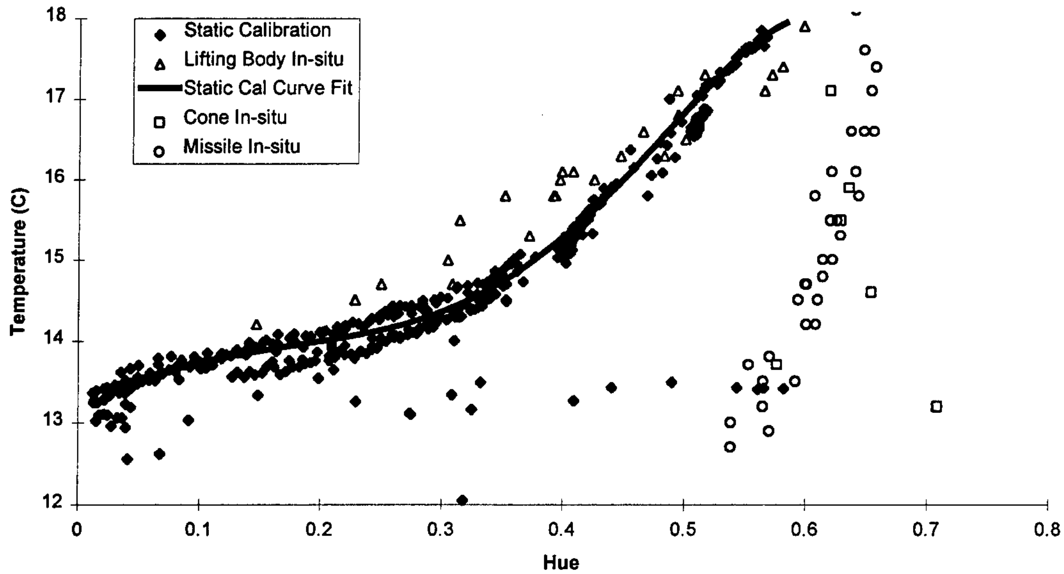

Figure 2a: 6C Static Calibration and In-Situ Measurements

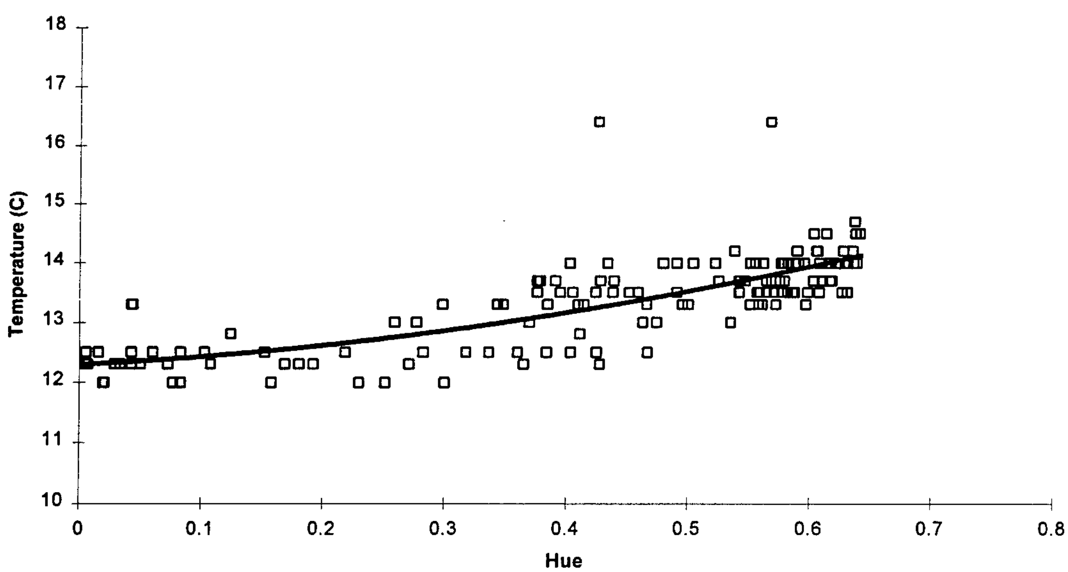

Figure 2b: 2C Static Calibration Curve

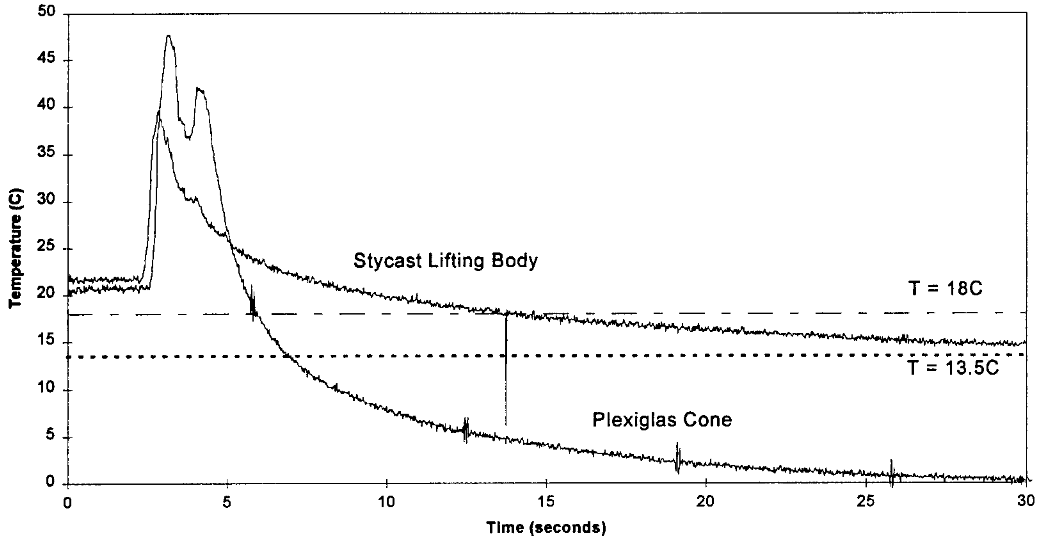

Figure 3: Cone Wall Temperature vs Time

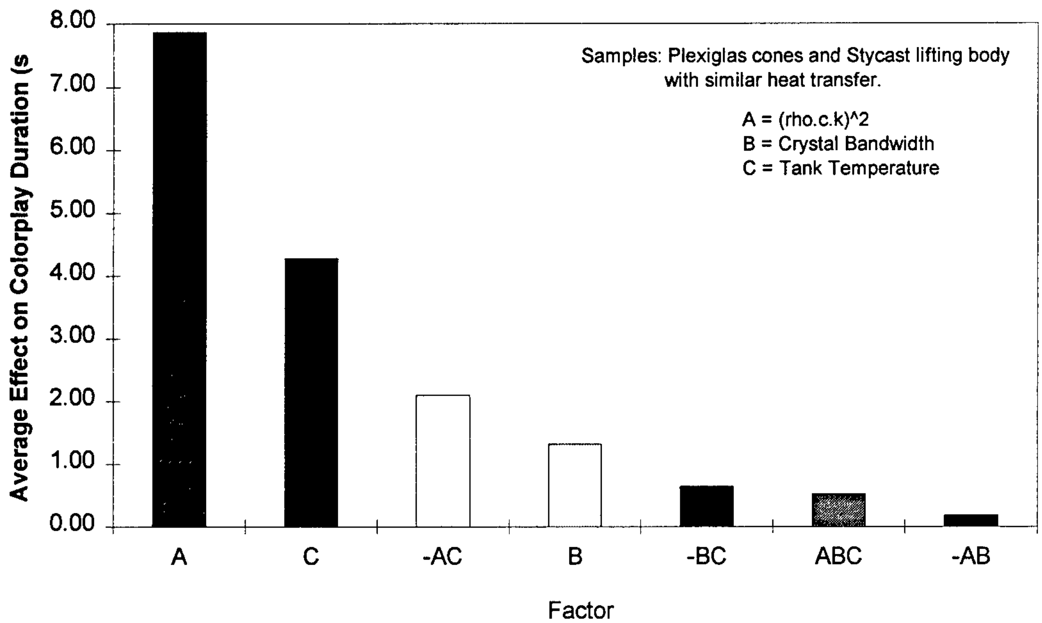

Figure 4a: Comparison of $(\rho ck)^2$, Bandwidth and Tank Temperature Effects on Colorplay Duration

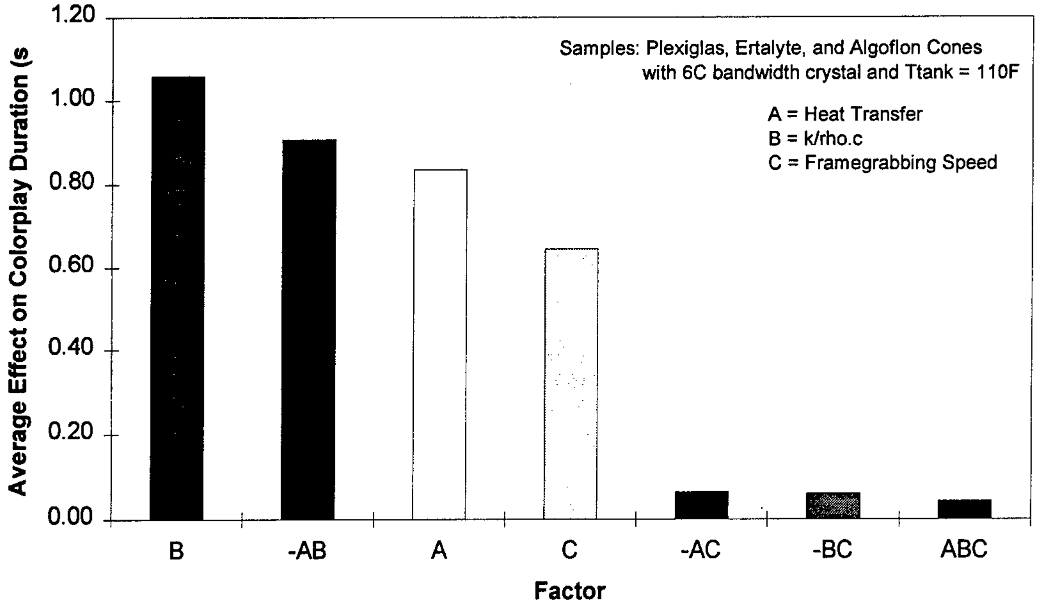

Figure 4b: Comparison of Heat Transfer, k/ρc, and Framegrabbing Speed Effects on Colorplay Duration

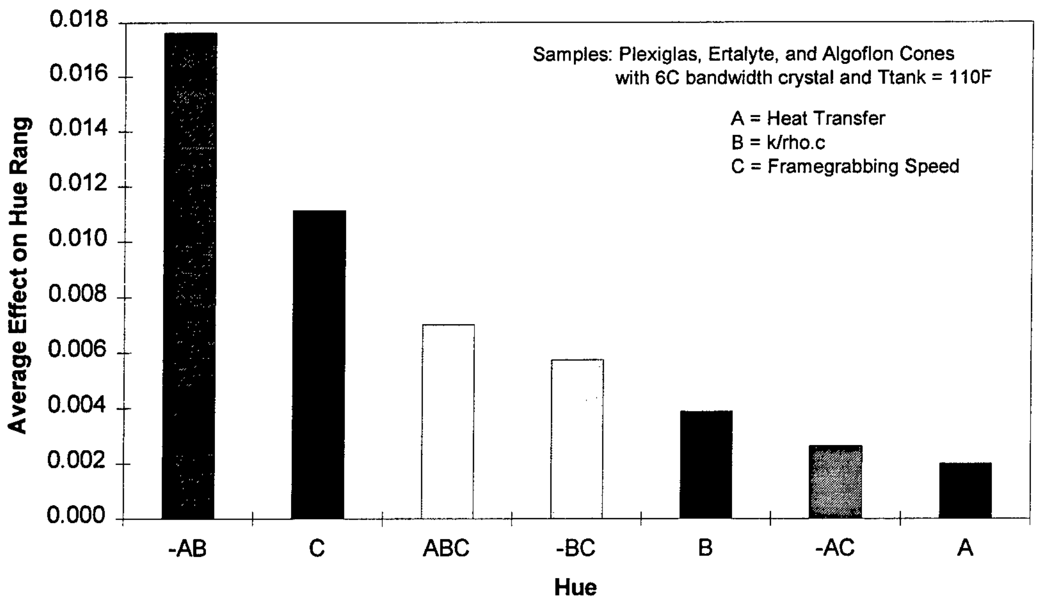

Figure 5: Comparison of Heat Transfer, k/ρc, and Framegrabbing Speed Effects on Hue Range

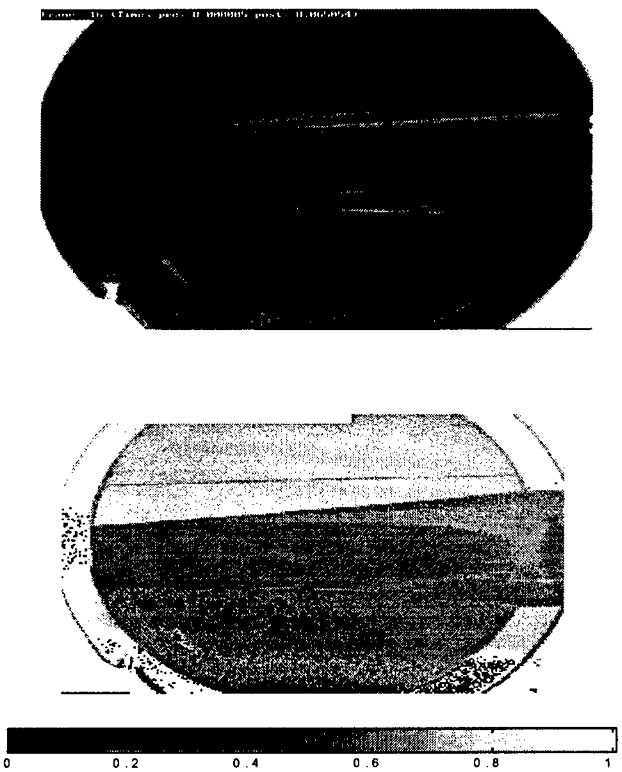

Figure 6: Colorplay Washout on Visual and Hue Images

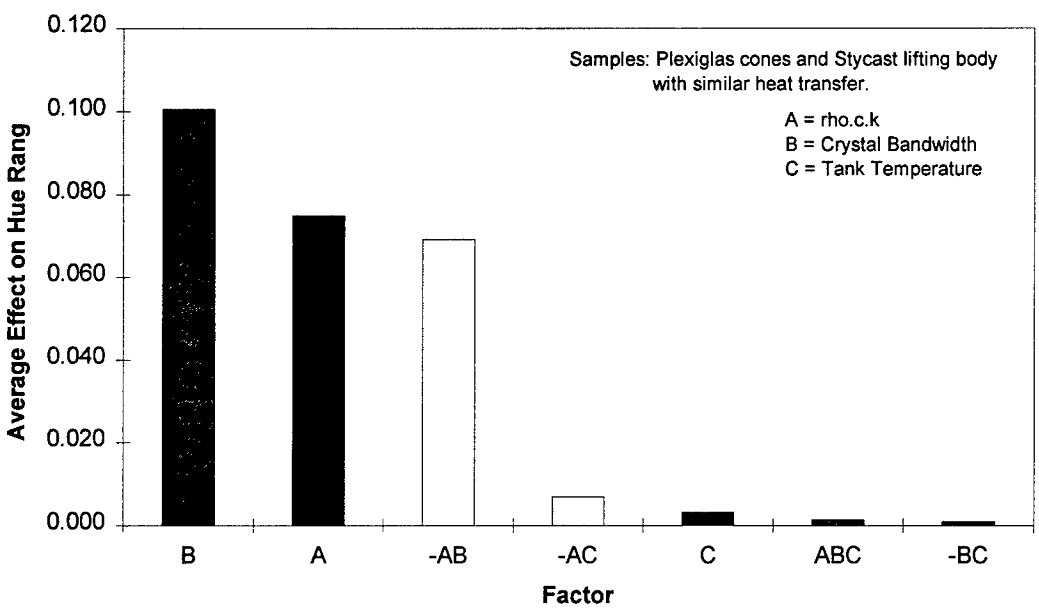

Figure 7: Comparison of $(\rho ck)^{1/2}$, Bandwidth and Tank Temperature Effects on Hue Range

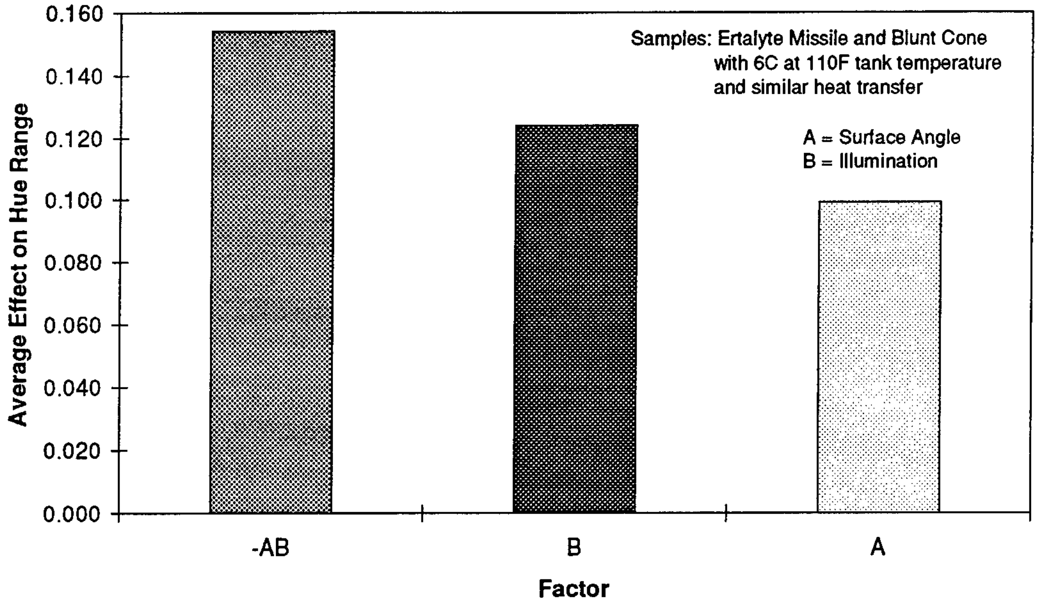

Figure 8: Comparison of Surface Angle land Illumination Effects on Hue Range

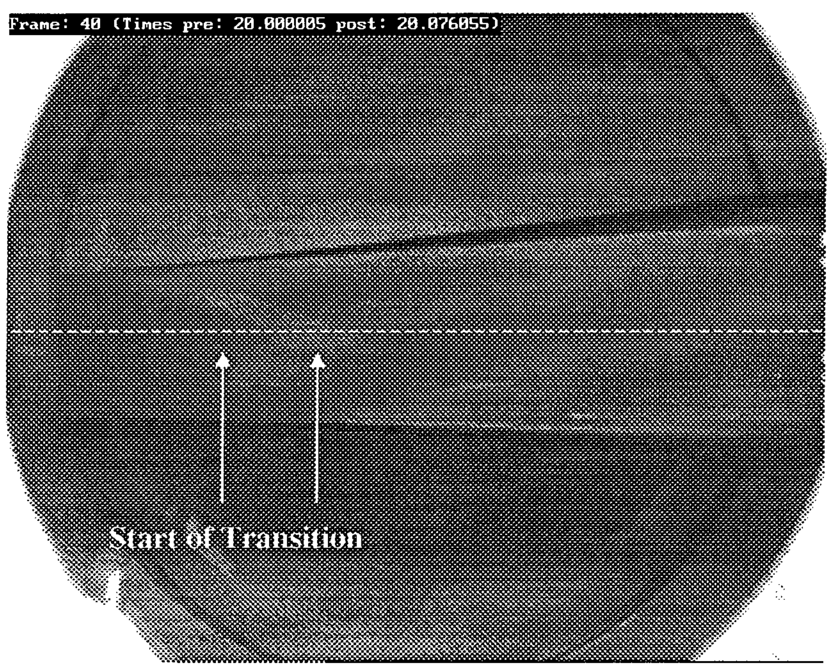

Figure 9: Identifying Boundary Layer Transition on API Model

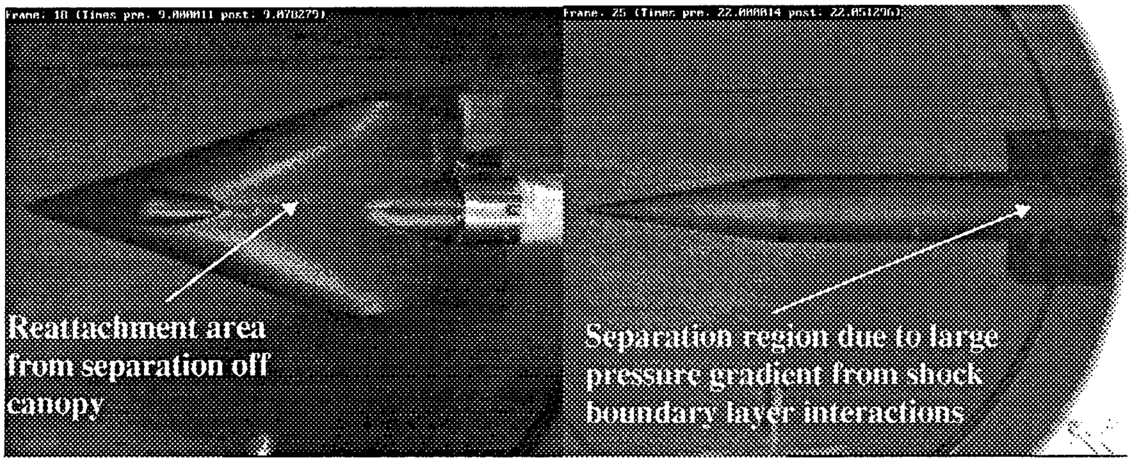

Figure 10: Liquid Crystal Indications of Boundary Layer Features

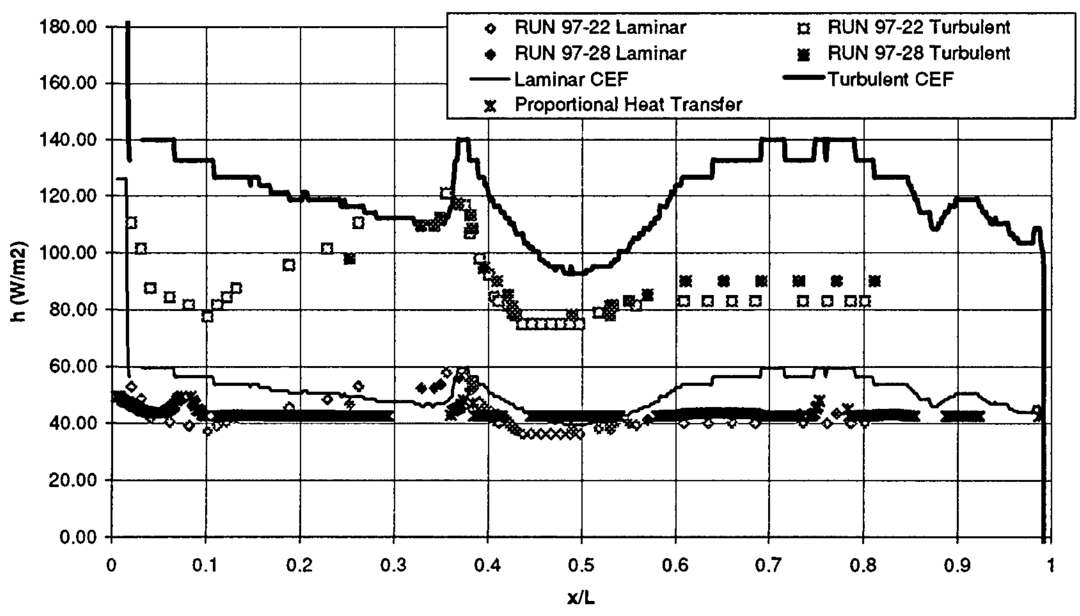

Figure 11: Comparison of Data Reduction Methods For Missile Model

A Setup for Photoassociation of Cold, Trapped Cesium Atoms

Bridget Mc Grath
Graduate Student
Department of Physics

University of Colorado at Colorado Springs
P.O. Box 7150
Colorado Springs, CO 80933-7150

Final Report for:
Summer Faculty Research Program
U.S. Air Force Academy

Sponsored By:
Air Force Office of Scientific research
Bolling Air Force Base, DC

and

U.S. Air Force Academy

September 1997

A SETUP FOR PHOTOASSOCIATION OF COLD, TRAPPED CESIUM ATOMS

Bridget McGrath
Department of Physics
University of Colorado at Colorado Springs

Abstract

An existing Magneto-Optical Trap (MOT) setup was modified to allow for photoassociation studies. A photoassociation laser was directed towards the trapping cell, and a system for molecule detection was installed, consisting of a photoionization laser, and channeltron detection. Initial attempts at photoassociation were unsuccessful, but work will continue in this area, now that the groundwork has been completed.

Introduction

In the past 10 years, successes in the field of laser trapping and cooling of atoms have furthered research into quantum effects and precision spectroscopy. As a next logical step, interest has turned to performing the same feat for molecules. This stems from the applications of cold molecules to developing better clocks and stabilized lasers. Laser cooling involved the repeated momentum exchange of many photons. However, the cycling transitions in the alkali atoms which allow for rapid absorption and emission of photons, necessary for cooling, are not available in molecules. Because of the molecules' additional rotational and vibrational degrees of freedom, there are no transitions which can be easily exploited in this fashion. A complicated scheme has been proposed for possible cooling of molecules. [1] Most of the recent research, however, has focused on the creation of cold molecules by photoassociation of already cooled and trapped atoms. [2, 3, 4, 5, 6]

Photoassociation studies of Li, K, Na, and Rb have allowed spectroscopy of the long range molecular states largesly inaccesible from bound molecular states. In this paper we report the results of an attempt to create cold Cesium molecules in the same fashion..

The majority of photoassociation studies use atoms trapped in a Magneto-Optical Trap (MOT). A MOT is comprised of basically two features. The first, known as optical molasses involved 3 counterpropagating laser beams tuned slightly to the red of the desired transition in the atom. Doppler shifts arising from an atoms motion will bring the laser light into resonance with the atom. Absorption of the photon gives the atom a momentum kick in the opposite direction of its initial velocity. The total effect is to slow the atoms within the laser beams. The second component of the MOT is a pair of Helmholtz coils. The magnetic field created by the current creates, via the Zeeman shift, a position-dependent force on the atoms. Thus the atoms are slowed and trapped.

In the photoassociation process, a photon is absorbed by a cold atom in close proximity to another. This can form an excited state bound molecule which will decay 90% of the time back into two atoms. Ten percent of the excited molecules will decay into a bound molecular ground state. Either case will result in a loss of atoms from the trap. Thus a photoassociation spectrum can be achieved by studying trap loss as a function of the frequency of the photoassociation laser, as has been in the previous studies. A second possible method for studying photoassotiation involves detecting the resultant molecules directly.

These molecules can be ionized by the absorption of another photon, and the ions can then be detected using an electron multiplier. [7] Time of flight analysis could then provide the means of differentiating atoms from molecules. A photoassociation spectrum can also be achieved in this manner. A further benefit of this approach is that, since the molecules have many more intermediate states than the atoms, photoionization is much more likely process, and saturation can easily be achieved for relatively low ionization laser intensities.

Methodology

Our setup consisted of a standard MOT with a background pressure of 10^{-10}Torr. The trapping beams come from an 852 nm diode laser locked to the cycling 4-5' transition by saturated absorption, with a series of acousto-optic modulators (AOM's) providing the detuning of 20 MHz. The repumping light is provided by another diode laser on the 894 nm F= 3-4 transition. Our magnetic field gradient is 10 Gauss/cm, and the MOT captures about 10^7 atoms at a density of 10^9 cm^{-3}.

In order to achieve a higher density, we modified the MOT by inserting dark spots into the center of the repumping beams, as first proposed by Ketterle et. al. . [8] This "dark spot " MOT confines the atoms in the central region of the trap to the "dark" F=1 hyperfine ground state, so that they cannot interact with the trapping laser, thereby reducing the outward radiation pressure at the center of the trap.

A pulsed frequency doubled ND:YAG laser (532 nm) ionizes the atoms and molecules, and the subsequent ions are collected and detected with a Channeltron electron multiplier.

Results

We initially performed a series of tests on the setup. With a two- photon process required for the ionization of Cesium, we expected that the Channeltron signal strength should increase as E^2 of the ionization laser. As seen in Fig. 1, we found an experimental slope of 1.5, when plotting the log of the signal size vs. The log of the energy.

Fig. 1
Ion Signal Size vs. Intensity

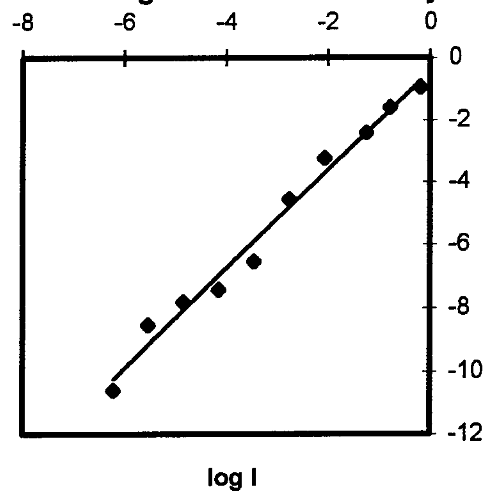

Following that we focused on distinguishing the molecular signal from the atomic signal, in preparation for later attempts at photoassociation. We found that the Cs ions reached the detector between 25 and 30 microseconds after the laser pulse (Fig. 2)., in agreement with our computer simulation for the setup. Even without photoassociation, we expect a certain number (about 1%) of naturally occurring molecules in the trap. These would almost all be ionized at our laser power, and collected by the Channeltron. There is indeed a smaller peak occurring at a factor of $2^{1/2}$ later in time of flight. Identifying this definitively as the molecular peak, however, gives rise to several problems.

Fig. 2
Histogram of Pulse Frequency vs. Time of Flight

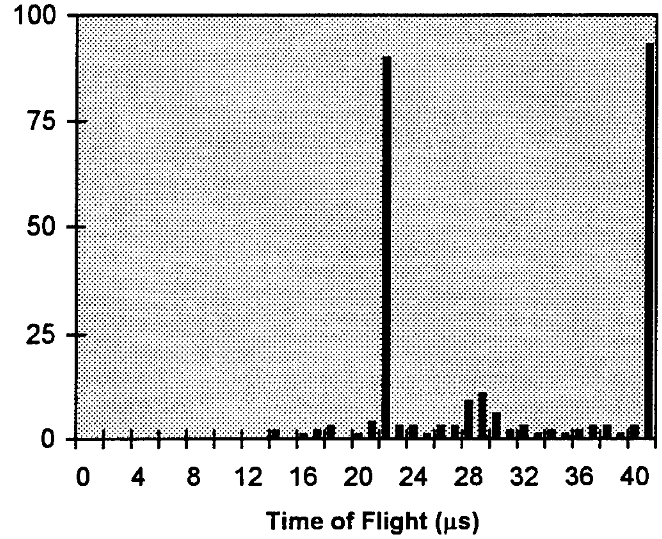

First, there is also a third, much larger peak, occurring later, for which we have no solid explanation. It is possible that this is the result of ionization of Cesium from the walls of the cell, but we are far from certain. Secondly, as the intensity of the ionization laser is reduced, one would expect the atomic peak to fall off sharply, while the molecular peak would be relatively unaffected, due to saturation. This, however, was not the case. We found that when the intensity was reduced by a factor of 10, the frequency of ionizations per pulse for atoms decreased by a factor of 100, as predicted. The molecular peak, on the other hand, experienced a frequency reduction by a factor of 10,000.

Finally, it was difficult to get consistent data. As mentioned above, the time of the atomic peak varied in different runs, making the expected time of a molecular peak difficult to identify. We believe that part of the problem lies in the stability of our MOT. Further modifications to the setup, such as locking the 894 laser with saturated absorption, and redesigning the cell, should provide the needed stability. Attempts at photoassociation were unsuccessful. Nevertheless, the groundwork for further studies has been completed.

References

[1] J. T. Bahns, W. C. Stwalley, and P. L. Gould, J. Chem. Phys. **104**, 9689 (1996).

[2] Y. B. Band, and P. S. Julienne, Phys. Rev. A **51**, R4317 (1994).

[3] P. A. Molenaar, P. van der Straten, and H. G. M. Heideman, Phys. Rev. Lett. **77**, 1460 (1996).

[4] J. D. Miller, R. A. cline, and D. J. Heinzen, Phys. Rev. Lett. **71**, 2204 (1993).

[5] P. D. Lett, K. Helmerson, W. D. Phillips, L. P. Ratliff, S. L. Roston, and M. E. Wagshul, Phys. Rev. Lett. **71**, 2200 (1993).

[6] H. Wang, P. L. Gould, and W. C. Stwalley, Phys. Rev. A **53**, R1216 (1996).

[7] P. L. Gould, P. D. Lett, P. S. Julienne, and W. D. Phillips, Phys. Rev. Lett. **60**, 788 (1988).

[8] W. Ketterle, K. B. Davis, M. A. Joffe, A. Martin, and D. E. Pritchard, Phys. Rev. Lett. **70**, 2253 (1993).

RELATIONSHIP BETWEEN GROWTH HORMONE AND MYELIN BASIC PROTEIN EXPRESSION *IN VIVO*

Donna M. Lehman
Graduate Student
Department of Cellular and Structural Biology

The University of Texas Health Science Center at San Antonio
7703 Floyd Curl Drive
San Antonio, Texas 78284

Final Report for:
Graduate Student Research Program
Clinical Investigations Division, Wilford Hall

Sponsored by:
Air Force of Office of Scientific Research
Bolling Air Force Base, DC

and

Wilford Hall

September 1997

RELATIONSHIP BETWEEN GROWTH HORMONE AND MYELIN BASIC PROTEIN EXPRESSION *IN VIVO*

Donna M. Lehman
Graduate Student
Department of Cellular and Structural Biology
The University of Texas Health Science Center at San Antonio

ABSTRACT

Proper functioning of the mammalian nervous system requires myelination of neuronal axons. Myelination of the newborn mouse brain begins shortly after birth and is complete by about 20 days of age. Abnormalities of myelin basic protein (MBP) production have a direct impact on myelination as has been demonstrated in the shiverer mouse. Mice with less than 25% of normal MBP levels have aberrant myelination and brain development and demonstrate a characteristic tremor at 12 days of age. Growth hormone (GH) and insulin-like growth factor I (IGF-1) have been shown *in vitro* and *in vivo* to affect myelination. This project explores the effect of GH deficiency on myelin basic protein expression to determine whether the GH deficiency exacerbates MBP haploinsufficiency. These studies grew out of studies undertaken on children with 18q- syndrome who have only a single copy of the MBP gene, are hypomyelinated, and are also shown to suffer growth hormone deficiency or insufficiency. A hybrid mouse model which mimics these deficiencies of 18q- patients is being developed to explore the reltationship between GH and MBP *in vivo*.

RELATIONSHIP BETWEEN GROWTH HORMONE AND MYELIN BASIC PROTEIN EXPRESSION *IN VIVO*

Donna M. Lehman

INTRODUCTION

Expression of the myelin basic protein (MBP) gene is critical for normal myelination of the central nervous system (CNS). This has been most clearly demonstrated by the neuropathology of the mutant shiverer (*shi/shi*) mouse in which a large portion of the MBP gene is deleted and MBP protein is essentially undetectable (1,2). Consequently, the CNS has virtually no compact myelin. These mutants exhibit a characteristic tremor (shiver) appearing at 12 days of age, coincident with the normal age at which myelination occurs in rodents, and die prematurely usually during status epilepticus. That MBP deficiency is responsible for the phenotype is supported by mutant rescue with a MBP transgene (3).

Cross-beeding experiments utilizing mice transgenic for the MBP gene have established the level of MBP expression sufficient for normal myelinogenesis (4). Heterozygous shiverer mice produce about 50% of the normal level of MBP mRNA and a proportionate amount of MBP protein. These animals exhibit a normal behavioral and morphological phenotype; however, they have minor biochemical changes in myelin composition. Mice which express less than 25% of MBP display the shivering of the dysmyelinating phenotype. These data indicate that the level of MBP expression influences the assembly of myelin by oligodendrocytes which suggests that factors which influence MBP expression also influence myelin synthesis and assembly. Additionally, factors which regulate oligodendroglial proliferation and differentiation may affect myelinogenesis. In this regard, there is much evidence, both *in vivo* and *in vitro*, that growth hormone (GH) and insulin-like growth factor 1 (IGF-1) enhance myelination (5,6,7,8). GH-deficient mice, such as the little (*lit/lit*) mutant which has an abnormality of the GH-releasing hormone receptor (Ghrhr) (9), are hypomyelinated; the hypomyelination is corrected by early postnatal GH treatment (10).

Based on these observations, GH may be a potentiator of MBP production. To test this, we have begun to examine the impact of naturally occurring GH deficiency (*lit/lit*) on MBP *in vivo*, to investigate the effects of MBP deficiency (*shi/shi*) on GH production, and to explore the relationship between GH and MBP in a hybrid mouse (*lit/lit, +/shi*) model. If GH affects MBP production, then MBP levels which are already reduced in the *+/shi* mouse may be further reduced in the GH-deficient hybrid, and therefore, the affected mice may display the dysmyelinating phenotype. Early treatment with GH may delay or prevent the appearance of the tremor. Alterations in developmental progression of myelination and its impact on function are being investigated.

These studies in mice grew out of studies undertaken on children with 18q- syndrome (11,12,13). The characteristic features of this syndrome are short stature, mental retardation and deafness. Affected children have only a single copy of the MBP gene and are hypomyelinated as demonstrated by quantitative magnetic resonance relaxometry (14). Half of affected children are GH-deficient and the other children have evidence of dysregulation of GH production. Accumulating human data suggest that GH treatment may improve both myelination and cognitive function (unpublished) raising the possibility that a relationship exists between MBP and GH. These mouse studies permit the opportunity to more thoroughly explore the relationship between GH and MBP within the context of the developing brain and may provide insight into novel treatment approaches to children with hypomyelination.

METHODOLOGY

Mouse colony: Little and shiverer mutant mice were supplied by Jackson Laboratory. The little mutant is in the C57Bl/6J background, and the shiverer mutant is in the C3H background. Wild-type little males were crossed with *lit/lit* females, and the heterozygous offspring (F1) were interbred to create +/+, *lit/+*, and *lit/lit* genotypes. C3H shiverer mice were also interbred to produce C3H mice for study. The hybrid mouse (*lit/lit;shi/+*) was produced by first crossing C57Bl *lit/lit* females with C3H *shi/shi* males to produce a double heterozygote. Male F1 mice were backcrossed to C57Bl *lit/lit* females.

Mutant genotyping: A method was developed to genotype the little locus (ghrhr) by PCR and subsequent restriction analysis (15). The shiverer locus (MBP) was determined by Southern analysis as previously published (16). A 581-bp probe which spanned the deletion breakpoint was designed for this purpose.

MBP quantitation: MBP mRNA and protein levels were assayed in each mouse. Brains were removed from mice; the right hemisphere was processed for RNA and the left hemisphere was frozen in liquid nitrogen and stored at -70°C for protein analysis by RIA. MBP mRNA levels were determined by Northern analysis. Total RNA was isolated from brain tissue using a protocol adapted from Chomczynski and Sacchi (17). Five μg of total RNA were electrophoresed through a 1.2% agarose gel. The blot was hybridized with a radiolabeled cDNA probe for the 14kD form of mouse MBP (gift of Dr. Carol Readhead). An α-tubulin probe was subsequently used as an internal control for normalizing the amount of RNA loaded. Quantitation was done with a phosphorimager.

IGF-1 and GH quantitation: Blood was collected from mice by cardiac puncture. Serum was separated from the cellular components and frozen. Fifty μl of serum was used per assay; assays were performed in duplicate. Each sample was acid-extracted using C-18 cartridges (Sep-Pak, Waters Associates) and IGF-1 assayed by radioimmunoassay. Serum assay of IGF-1 was performed by Dr. Ross Clark at Genentech, Inc. Anterior pituitaries were harvested for analysis of intrapituitary GH and stored at -70°C in sterile saline.

Auditory Brainstem Evoked Responses (ABR): ABRs were recorded using a Bio-Logic Navigator system. The mice were anesthetized with inhaled 1.5% isoflurane in 60% O_2. One hundred microsecond clicks are generated at a repetitive rate of 11.4/sec as the sound stimulation and then delivered by earphone to an external ear canal of the mouse through a 20 cm connecting tube. The evoked potentials, taken with needle electrodes inserted at the vertex and the ipsilateral paw, were amplified X 10^4, filtered with a band pass between 150 and 1500 Hz, and averaged from a total of 1000 click-evoked responses for the first 10 msec period following stimulation. The minimum detectable values on the two different points of the latency, measured by the cursor mode of the system, is 0.04 msec. The minimal hearing thresholds can be determined by 5 dB step sound stimulations according to the visually detectable amplitude of the first peak.

RESULTS

MBP levels in brain from little mice

Although there is extensive data on the effect of GH/IGF-1 on myelination, there is no information on the specific effect of GH/IGF-1 on MBP *in vivo*. The period of maximal MBP expression in mice is between 10 and 30 days after birth with the peak at about 15 days (18). Thereafter, expression declines and plateaus at a much lower level. Therefore, MBP expression was determined at 18, 25 and 60 days postnatal in little mice. The data for 25-day mice is complete and show that *lit/lit* mice have less MBP mRNA than controls ($p < 0.05$, +/+ vs. *lit/lit*) (Fig 1). This result suggests that a mechanism by which GH affects myelination is by altering the amount of MBP mRNA. The manner in which this is accomplished is unknown. MBP protein assays are in progress.

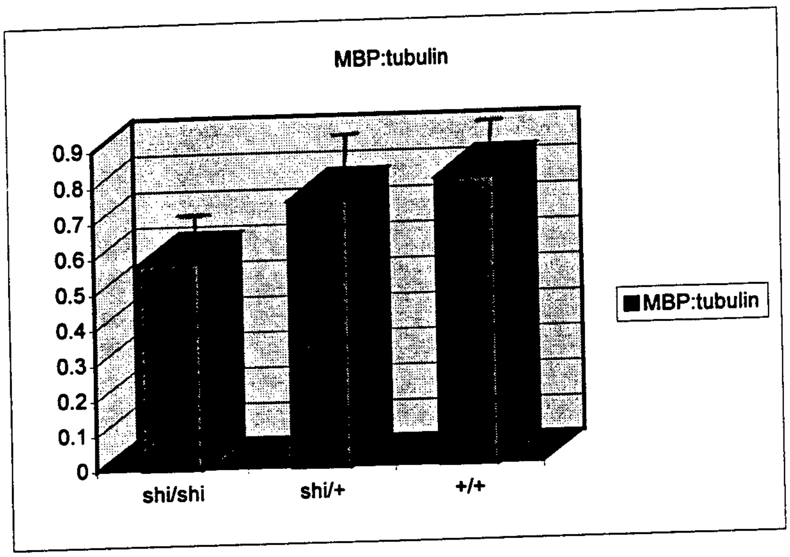

Figure 1. Quantitation of MBP mRNA in 25-day lit mice. Data are shown as a ratio of MBP mRNA to α-tubulin mRNA.

<u>Functional evaluation of myelination</u>

Alterations in the content or quality of myelin should have an impact on neural function. Auditory brainstem evoked responses were analyzed in several 2-month old mice at 90, 80, 70, 60, 50, 45 and 40 dbl: ABRs for 2 controls (C57Bl/6 +/+), 2 heterozygotes *(+/lit)* and 2 littles (*lit/lit*) at 90 dbl are shown in figure 2. Wave responses were also recorded from homozygous shiverer (*shi/shi*) mice for comparison. These results show that there are distinct differences between the controls, heterozygotes and little animals. Analysis of the evoked responses revealed a Wave 1 in *lit/lit* mice that had a normal amplitude, latency and morphology; in all animals tested, the remainder of the waveform lacked identifiable peaks. These data suggest that there is normal cochlear and VIIIth nerve function and abnormal auditory brainstem function in *lit/lit* mice. Whether the differences in ABR are due to hypomyelination is not yet clear; however, it is intriguing to consider that there is a relationship between GH deficiency, hypomyelination and hearing. It is noteworthy that homozygous shiverer and homozygous little mice also have distinct responses. This could indicate that either their degrees or basis of hypomyelination differ. Ultrastructural assay of the auditory nerve, such as by electron microscopy, may provide answers. Nonetheless, this functional assay can distinguish these genotypes which is helpful when studying the hybrid mouse model (*lit/lit;shi/+*).

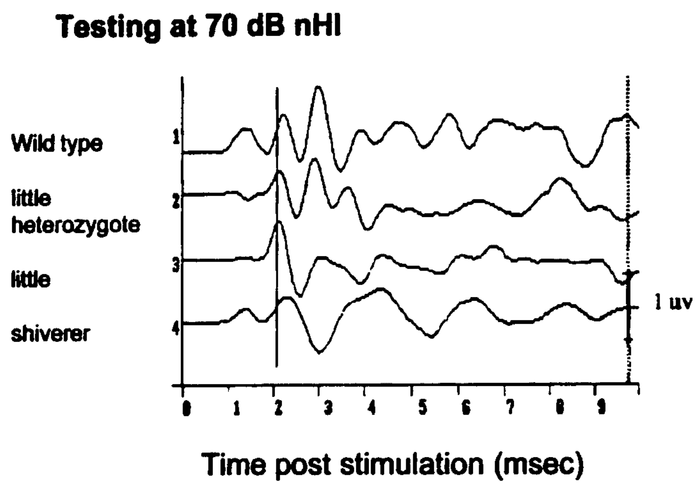

Figure 2. Auditory brainstem evoked responses in lit mice.

Circulating IGF-1 levels in shiverer mice

No information is available on the impact of the shiverer mutation on the neuroendocrine axis. Because of interest in the potential effect of an abnormality of MBP on GH production, serum IGF-1 of 42-day old shiverer and control mice was assayed (Table 1). Due to the pulsatile nature of GH secretion, random serum GH determination does not provide useful information; therefore, IGF-1 was chosen as an initial marker for GH production. Since the number of 42-day old control animals is small, statistical evaluation could not be undertaken; however, a trend is apparent. Assays on additional animals may make these data significant. The functional significance of these changes on parameters other than somatic growth has not been evaluated. Pituitaries have been gathered for analysis of intrapituitary GH.

Genotype	***shi/shi***	***+/shi***	***+/+***
IGF-1 (ng/ml)	421 ± 104	552 ± 135	650 ± 99
(n)	(10)	(13)	(2)

Table 1. IGF-1 levels in shiverer mice and controls

Development of hybrid mouse model

We have demonstrated that the hybrid (*lit/lit; +/shi*) is viable. Studies are being conducted to establish the level of MBP expression and myelination in these hybrids and to determine if this differs from the *+/+; +/shi* and the *lit/lit;+/+* mice during development. The functional consequences of these changes will also be investigated.

DISCUSSION

GH-deficient little mice have previously been shown to be hypomyelinated (10), but the mechanism remains unclear. Our data indicate that MBP deficiency may be a factor. Homozygous little mice have only about 72% of MBP mRNA levels of control mice. MBP protein assays are in progress.

Auditory evoked brainstem responses have been used as a functional measure of myelination in shiverer mutants (19) as well as humans. We've shown that ABRs of little mutants are abnormal in that signal processing beyond the cochlea is disrupted. Very little data is available concerning GH-deficiency and auditory neurosensory impairment. This data may provide insight into the cause of abnormal ABRs in some 18q- children as well as potential therapy. Ultrastructural imaging of the myelinaton of the auditory nerve in little mice should prove useful in determining the cause of the aberrant ABRs.

18q- patients are haploinsufficient for MBP, but their cause of GH-insufficiency is unknown. The GH-insufficiency region on chromosome 18 has been narrowed (12), and the MBP gene lies within this region. To determine whether MBP could be a candidate gene for GH-deficiency/insufficiency in 18q- syndrome, we measured serum IGF-1 and intrapituitary GH levels in shiverer mutant mice and controls. The IGF-1 data indicate that homozygous shiverer mice have reduced circulating levels of this factor at 42 days. Since the number of control animals is small, statistical significance could not be determined. Assays on additional animals are underway. Also, intrapituitary GH analyses are in progress.

Development of a hybrid mouse model which has only one copy of the MBP gene in a GH-deficient background should prove useful in examining the relationship between GH and MBP production *in vivo*. We have shown that this hybrid is viable and are initiating studies to determine the consequences of GH-deficiency on MBP haploinsufficiency.

REFERENCES

1. Barbarese, E. et al. The effect of the shiverer mutation on myelin basic protein expression in homozygous and heterozygous mouse brain. J. Neurochem. 40(6): 1680-1686, 1983.

2. Roth, H.J. et al. Expression of myelin basic protein genes in several dysmyelinating mouse mutants during early postnatal brain development. J. Neurochem. 45(2): 572-580, 1985.

3. Readhead, C. et al. Expression of a myelin basic protein gene in transgenic shiverer mice: correction of the dysmyelinating phenotype. Cell 48: 709-712, 1987.

4. Popko, B. et al. Myelin deficient mice: expression of myelin basic protein and generation of mice with varying levels of myelin. Cell 48: 713-721, 1987.

5. Almazan, G. et al. Epidermal growth factor and bovine growth hormone stimulate differentitaion and myelination of brain cell aggregates in culture. Develop. Brain Res. 21: 257-264, 1985.

6. Beck, K.D. et al. Igf1 gene disruption results in reduced brain size, CNS hypomyelination, and loss of hippocampal granule and striatal parvalbumin-containing neurons. Neuron 14: 717-730, 1995.

7. Carson, M.J. et al. Insulin-like growth factor I increases brain growth and central nervous system myelination in transgenic mice. Neuron 10: 729-740, 1993.

8. Mozell, R.L. et al. Insulin-like growth factor I stimulates oligodendrocyte development and myelination in rat brain aggregate cultures. J. Neurosci. Res. 30: 382-390, 1991.

9. Godfrey, P. et al. GHRH receptor of little mice contains a missense mutation in the extracellular domain that disrupts receptor function. Nature Genet. 4: 227-232, 1993.

10. Noguchi, T. Effects of growth hormone on cerebral development: morphological studies. Hormone Res. 45: 5-17, 1996.

11. Ghidoni, D.P. et al. Growth hormone deficiency associated with the 18q- syndrome. Amer. J. Med. Genet. 69: 7-12, 1997.

12. Cody, J.D. et al. Growth hormone insufficiency associated with haploinsufficiency at 18q23. Amer. J. Med. Genet. 71: 420-425, 1997.

13. Hale, D.E. Growth failure and growth hormone deficiency in 18q- syndrome. Pediatr. Res. 37: 90A, 1995.

14. Gay, C.T. Magnetic resonance imaging demonstrates incomplete myelination in the 18q- syndrome. Evidence for myelin basic protein haploinsufficiency. Neuropsyc. Genet. 74: 422-431, 1997.

15. Lehman, D.M. et al. Rapid typing of the little mouse mutation. Mouse Genome 95(3): in press, 1997.

16. Molineaux, S.M. et al. Recombination within the myelin basic protein gene created the dysmyelinating shiverer mouse mutation. PNAS 83: 7542-7546, 1986.

17. Chomcynshi, P. and Sacchi, N. Single-step method of RNA isolation by acid guanidinium thiocyanate-pheno-chloroform extraction. Analyt. Biochem. 162: 156-159, 1987.

18. Carson, J.H. et al. Developmental regulation of myelin basic protein expression in mouse brain. Develop. Biol. 96: 485-492, 1983.

19. Fujiyoshi, T. et al. Restoration of brain stem auditory-evoked potentials by gene transfer in shiverer mice. Ann. Otol. Rhinol. Laryngol. 103: 449-456, 1994.